Microporous and Mesoporous Materials 312 (2021) 110774

Contents lists available at ScienceDirect

Microporous and Mesoporous Materials

journal homepage: http://www.elsevier.com/locate/micromeso

Exploiting mesoporous silica nanoparticles as versatile drug carriers for several routes of administration

Rafael Miguel Sábio [a,*], Andréia Bagliotti Meneguin [a], Aline Martins dos Santos [a], Andreia Sofia Monteiro [b], Marlus Chorilli [a]

[a] School of Pharmaceutical Sciences - São Paulo State University (UNESP), 14800-903, Araraquara, São Paulo, Brazil
[b] Institute of Chemistry - São Paulo State University (UNESP), 14800-060, Araraquara, São Paulo, Brazil

ARTICLE INFO

Keywords:
Mesoporous silica nanoparticles (MSNs)
Administration routes
Drug delivery systems
Biological behavior

ABSTRACT

The exploitation of mesoporous silica nanoparticles (MSNs) as drug delivery systems has grown exponentially due to their remarkable tunable properties, such as high surface area, chemical and physical stability, high loading and release capacities, distinct possibilities of particle and pore structures, as well as good biocompatibility, biodegradability, and easy clearance. However, the main exposure routes that exploit MSNs qualities, namely intravenous, subcutaneous, intramuscular, intratumoral, ophthalmic, pulmonary, nasal, dermal, and oral administrations, have been underreported to date. In addition, a better understanding of these administration routes can contribute to the development of smart MSNs-based nanoplatforms with interesting properties, such as high stability in physiological media, specificity and efficacy in theranostic applications, and further clinical translations. This review highlights the advantages and challenges of the administration routes aforementioned regarding the MSNs as drug delivery systems. It also shows how their properties can influence the interaction with biological media, and consequently, their biocompatibility, biodistribution, and clearance mostly in preclinical assays, in order to contribute to further MSNs-based nanoplatform clinical translations.

1. Introduction

The research and design of nanomaterials has grown substantially to meet the needs of applications in the diverse fields of medicine, consumer products, environmental health, and information technology [1–3]. Nanomaterials consist of materials with one of their dimensions up to 100 nm. Great attention has been given to nanomaterials for biomedical applications, such as sensing, imaging, therapeutic, and theranostic agents [2–5].

Regarding therapeutic agents, organic and inorganic nanomaterials have been extensively applied as active drug carriers to develop novel drug delivery systems, and consequently, novel vaccine formulations due to their tunable physicochemical properties, such as wide availability, rich functionality, and interesting biocompatibility [4,6]. Besides, these engineered materials display small size and high surface area, which allows good interaction with single cells aiming to mimic natural and biological systems, such as lipids, sugars, peptides, nucleic acids, and others. These nanosystems usually show advantages such as long circulation times in blood and biological media, few unspecific interactions, and therefore, high specificity for designed target cells and tissues [2,4].

Among several nanomaterials, mesoporous silica nanoparticles (MSNs) have attracted great attention as drug delivery nanoplatforms due to their unique properties, namely high chemical and thermal stability, high surface area, tailorable particle and pore sizes as well as shapes. The pore structure can promote drug confinement, controlling loading and release processes, and avoiding drug degradation and premature release before reaching the target. In addition, the hydroxyl groups available in MSNs surface (exterior and interior of the pores) can be easily functionalized, making MSNs interesting multifunctional nanocarriers for biomedical applications [4,7–10].

Most MSNs can be prepared using mild and cheap processes by controlling parameters such as reagent concentration, temperature and pH of the reaction mixture, template agents (surfactants and copolymers), and types of silica source [4]. As stated by some authors [4, 11–15], MSNs biomedical applications are extremely dependent on the

* Corresponding author.
E-mail addresses: rafael.m.sabio@unesp.br (R.M. Sábio), abagliottim@hotmail.com (A.B. Meneguin), aline.martinsdossantos@yahoo.com.br (A. Martins dos Santos), monteiro.andreia87@gmail.com (A.S. Monteiro), marlus.chorilli@unesp.br (M. Chorilli).

https://doi.org/10.1016/j.micromeso.2020.110774
Received 8 July 2020; Received in revised form 26 October 2020; Accepted 19 November 2020
Available online 22 November 2020
1387-1811/

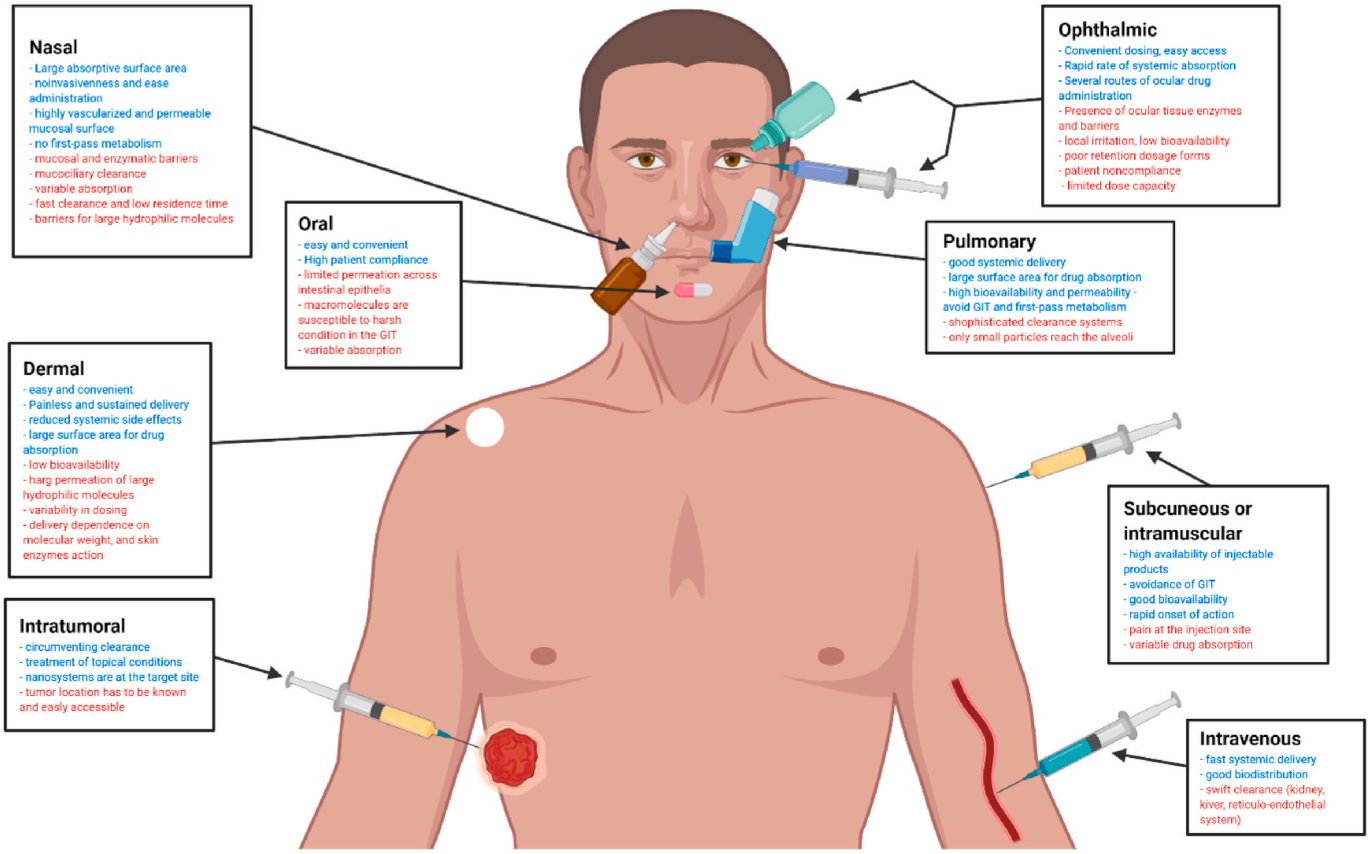

Fig. 1. Schematic representation of exposure routes commonly used for MSNs administration, including their main advantages (blue) and challenges (red). (For interpretation of the references to color in this figure legend, the reader is referred to the Web version of this article.)

biological media response compared with factors such as particle dosage, particle shape and surface, mesoporous structure, pore and particle size.

Although several *in vitro* [7,12,16–21] and *in vivo* [4,14,22–28] studies have proved good biocompatibility of pristine and engineered MSNs, few clinical trials have reported the effects of MSNs, administered via distinct routes, on the complete clearance from human organisms. The possible routes of exposure by using MSNs as nanoplatforms comprise intravenous, subcutaneous, intramuscular, intratumoral, ophthalmic, pulmonary, nasal, dermal, and oral administration.

Taking into account that reviews concerning distinct administration routes for MSNs are scarce, we proposed to highlight the advantages and challenges of the exposure routes most commonly used for these nanoplatforms as drug delivery systems. We also review how MSNs properties can influence the interaction with biological media, and consequently, their biocompatibility, biodistribution, and clearance *in vivo,* in order to contribute to further MSNs clinical applications.

2. Mesoporous silica nanoparticles

Mesoporous silica materials comprise materials with high surface area due to diameter pore size from 2 to 50 nm, as stated by International Union of Pure and Applied Chemistry (IUPAC) classification [9,29]. In particular, MSNs were first reported by some authors [30–32] who adapted the Stöber method [33] with surfactants or copolymers as organic templates, alcohol solution in basic media (by addition of ammonium hydroxide or sodium hydroxide) and then, a silica precursor to form organic-inorganic hybrid structures. Parameters such as reagent type and concentration, pH and temperature can influence particle size and shape, along with pore size and assembly, to fabricate MSNs [4,9,34,35]. Briefly, a general MSNs synthetic route comprises two mechanisms: true liquid-crystal templating (TLCT) and cooperative self-assembly. The TLCT mechanism consists of the micellar aggregate formation by self-assembly of surfactants or copolymers at high concentration and specific media conditions. Then, the inorganic source (tetraethyl-orto silicates [TEOS]) is precipitated onto periodic micellar assembly. In the cooperative self-assembly mechanism, the silica precursor promotes the surfactant assembly at low concentration to prepare mesostructured systems [4,30,36,37]. The organic templates can be removed by calcination, solvent extraction, or dialysis, making silica mesopores free (internal surface) for active molecule confinement and, consequently, further biomedical applications.

3. Distinct administration routes

Considering MSNs as matrices for drug delivery, the great challenge of becoming an efficient nanoplatform to treat any disease comprises achieving high specificity, high blood circulation time, good cellular uptake, intracellular release, and short clearance time. Several multifunctional MSNs have been described aiming to achieve the attributes mentioned above, minimizing side effects on healthy tissues and cells [4,38]. Regarding clinical applications, it is worth emphasizing that knowing the administration routes and their implications is essential for designing targeted MSNs as efficient drug delivery systems. In this sense, we review the exploitation of MSNs as drug carriers by using several administration routes, showing their advantages and challenges, as summarized in Fig. 1. The main findings concerning the fate of the administered nanosystems, from toxicity and biodistribution to clearance, are highlighted here.

The choice of administration route depends on the disease, the effect desired, and the products available to achieve the goal. The MSNs multifunctionality opens new horizons to design targeted drug

Table 1
Summary of several administration routes for MSNs as drug carriers, types of MSNs-based nanoplatforms, their physicochemical parameters, and main results.

Administration routes	Carriers/composition	Drugs	Encapsulation efficiency (%)	Particle size (nm)	Pore size (nm)	Zeta potential (mV)	Main results/goal	Reference
Intravenous	Anti-PSA-NCAM-PE (antibody)-UnPSi NPs (modified porous silicon nanoparticles)	SC-79	23	358	–	−19	Targeted and drug delivery nanoplatform to stimulate the Akt pathway aiming at regenerating functional neurocircuitry after stroke.	[27]
Intravenous	Ru-MSN-P(target protein)lip (liposome)	RuDPNI ($C_{26}H_{19}Cl_3N_3O_3SRu$) and RuDPH ($C_{14}H_{14}Cl_3N_2OSRu$)	26.5	60	8.5	−10.5	Ru-MSN-PLip exhibited long-term blood circulation, biocompatibility, accumulation in tumors, and inhibition of tumor growth *in vivo*.	[39]
Intravenous	CuS@BSA (bovine serum albumin)-HMONs (hollow mesoporous organosilica nanoparticles)-DOX	Doxorubicin (DOX)	42.9	117.6	1.8	+21.3	CuS@BSA-HMONs-DOX exhibited pH-, NIR- and GSH-sensitive drug release, fulfilling synergistic chemo-phototherapy functions.	[40]
Intravenous	MYR-MRP-1 (multidrug resistance protein small interfering RNA [siRNA])/MSN-FA (folic acid)	Myricetin (MYR)	36.7	109.8	–	–	Clinical treatment of non-small cell lung cancer (NSCLC).	[41]
Intravenous	DOX/MCN (mesoporous carbon nanocomposite)@Si (mesoporous silica nanoparticles)-CDs(carbon dots)	DOX	48.2	118	2.2	−23	Theranostic nanosystems for efficient chemo-photothermal synergistic antitumor therapy.	[42]
Intravenous	MSN-SS (disulfide bound)-PDA(polydopamine)/DOX	DOX	19.4	150	2	−2	Multi-responsive drug delivery and combined chemo-photothermal therapy.	[43]
Intravenous	DMK NPs (DOX and KLAK peptide modified PEG loaded into mesoporous silica nanoparticles)	DOX and KLAK peptide	27.6 and 11.1, respectively	50	4.1	+15.5	Dual Redox/sensitive and controllable pH-responsive drug release behaviors showing high antitumor efficacy and high biosafety *in vivo*.	[44]
Intravenous and intratumoral	TAX-CUR-PL(PEGylated lipid bilayer) MSNs	paclitaxel (TAX) and curcumin (CUR)	77.5 and 30.7, respectively	130	2.7	–	Effectively reduce the clinical dosage of drugs and their toxic side effects, effectively carry drugs into cancer cells, and exhibit good targeting characteristics for breast cancer.	[45]
Intravenous	DOX/MSN@$CaCO_3$@CM(cancer cell membrane debris)	DOX	4.2	160	–	−19.8	Effective drug targeting system only using natural biomaterials for the treatment of prostate cancer.	[46]
Intravenous	MSN-ATZ-CH (chitosan)-FA	Anastrozole (ATZ)	52.5	168.9	3	+26.2	Excellent tumor suppressing activity against Ehrlich Ascites Carcinoma (EAC) induced breast cancer model.	[47]
Intravenous	BSA-MnO_2@HMSNs(hollow mesoporous silica nanosystem)-DOX-Ce6, labeled BMHDC	DOX and chlorine e6 (Ce6)	14 and 36, respectively	274	3.2	~ −20	A high DOX-loading, pH/GSH(glutathione)/H_2O_2-responsive nanoplatform to achieve intelligent chemotherapy and enhanced PDT for cancer treatment.	[48]
Intravenous	D(DOX)/C(Cypate)/PG(Glutamic acid modified Pluronic P123)MSN and D/C/P(Pluronic P123)MSN	DOX and Cypate	10.5 and 8.2, respectively	Up to 240 nm	2.4	0 and −20, respectively	pH and near-infrared (NIR) light dual-responsive DOX release. Besides, deep tumor penetration and targeted PTT effect made PGMSN suitable for cancers overexpressing LAT1 receptors.	[49]
Intravenous	T(D-α-tocopherol polyethylene glycol 1000 succinate) C(Cypate)MSN/DOX	DOX	Up to 10	~ 120	2.5	+20	The double inhibition of drug effluxand particle exocytosis in this nanosystem cocontributed to sustaining drug action time, enhancing the anti-tumor activity.	[50]
Intravenous	SiNPs/DOX	DOX	25	189	2.8	–	The nanoplatform improved the cellular drug delivery efficiency and exhibited high cytotoxicity, achieving the inhibition of tumor growth.	[51]
Intravenous	S(sphere like)-M(magnetic)-MSNs-P(PEG-g-PLL conjugation)@GCV@pTK(virus thymidine kinase)	Ganciclovir (GCV)	33.7	250	2.8	–	The fabricated nanosystems showed successful pTK/GCV delivery to perform combined suicide gene/magnetic hyperthermia therapy of hepatocellular carcinoma (HCC).	[52]
Intravenous	(MSN)/MoS2-PEG nanoparticles (SMPs)	DOX	64.7	147	3.7	+2.28	SMPs nanoplatform showed great synergistic effect, i.e., the heat produced during PTT can increase the chemotherapy sensitivity of DOX	[53]

(*continued on next page*)

Table 1 (*continued*)

Administration routes	Carriers/composition	Drugs	Encapsulation efficiency (%)	Particle size (nm)	Pore size (nm)	Zeta potential (mV)	Main results/goal	Reference
							and synergistically improve its therapeutic effect for cancer treatment.	
Intravenous	AC-CMC(acetylated carboxymethylcellulose)/HMSN	DOX	39	180	–	~ −20	AC-CMC/HMSN possess specificity, enhanced cellular uptake, and tumor growth inhibition, showing potential as a novel targeted vehicle for efficient delivery of chemotherapeutics to the tumor tissue.	[54]
Intravenous	PEG-spherical MONs (mesoporous organosilica nanoparticles)	DOX	–	20–40	1.8–3.8	–	MONs-based drug delivery systems with significantly enhanced antitumor effect and largely diminished systemic side effects on normal tissues and organs. Fabrication of MONs with reduction-responsive biodegradation behavior and high performance for drug delivery, with great potential for clinical translation.	[55]
Intravenous	C(celastrol)MSN-PEG	Celasterol (CST)	99.9	150	–	~ −32	CMSN-PEG was effectively used as a mitochondrial targeting system for efficient inhibition of solid tumors.	[56]
Intravenous	PMOs(periodic mesoporous organosilic)-DOX@MoS_2-PEI(polyethylenimine)-BSA-FA	DOX	18.5	314	3.8	+6.8	The nanoplatform displayed good biocompatibility and synergistic chemo-photothermal therapy, significantly inhibiting tumor growth, with great potential in cancer therapy.	[57][
Intravenous	^{89}Zr-b(bacterial like)GNR(gold nanorods)@MSN (DOX)-PEG	DOX	40.9	average length and width 104.6 and 68.6, respectively	4–8	−4.3	Theranostic nanoplatform for photoacoustic imaging-guided chemo-photothermal cancer therapy *in vivo*.	[58]
Intravenous	DOX@MSNs-TPGS (D-a-tocopheryl poly-ethylene glycol 1000 succinate copolymer)	DOX	92.65	160.3	–	–	High and specific cellular uptake (MCF-7/ADR cells) and noticeable *in vivo* anti-tumor efficacy.	[59]
Intravenous	ND-MMSNs (neutrophils capped DOX-loaded magnetic mesoporous silica nanoparticles)	DOX	94.5	75.3	3	–	D-MMSNs possess high drug loading efficiency and do not affect the host neutrophil viability, improving intratumoral drug concentration and delaying relapse of surgically treated glioma.	[60]
Subcutaneous	PEG-MSNPs-CUR	CUR	92.4	184.6	–	+20.8	Enhancement of Cur bioavailability, protection from premature degradation, leading to tumor growth inhibition, suggesting its application as therapeutic agent for clinical trials.	[61]
Subcutaneous	MSNs@OVA and CpG-ODNs plus MSRs(mesoporous silica microrods)@GM-CSF -MSNs	Ovalbumin (OVA) and CpG oligodeoxynucleotides (CpG-ODNs)	–	150	20–30	~ −12	MSR-MSN vaccine promoted the generation of a large number of cytotoxic antigen-specific T cells against cancer besides exhibiting enhanced antitumor prophylactic efficacy and animal survival rate compared to the precursor vaccine.	[62]
Subcutaneous	AIPH/MSN-TPP(triphenylphosphonium)@Lipo (liposome)/DTX-FA NPs	AIPH(2,2′-azobis[2-(2-imidazolin-2-yl) propane] dihydrochloride) and docetaxel (DTX)	31.2 and 63.3, respectively	87.8	2.76	−19.3	FA induced tumor-targeting, excellent mitochondria targeting ability, pH-responsive drug release, temperature-activated alkyl radicals burst in mitochondria, and rational drug combination.	[63]
Subcutaneous	DOX-Gd (Gadolinium)-mSiO_2-HA (hyaluronic acid), labeled DGMH nanoparticles	DOX	58.6	137	3	–	Simultaneous bio-imaging (Computed Tomography and Magnetic Resonance imaging) and chemotherapy for the lymphatic system.	[64]

(*continued on next page*)

Table 1 (*continued*)

Administration routes	Carriers/composition	Drugs	Encapsulation efficiency (%)	Particle size (nm)	Pore size (nm)	Zeta potential (mV)	Main results/goal	Reference
Subcutaneous and intravenous	TOPSi (thermal oxidation of PSi), UnTHCPSi (1-undecylenic acid attached to THCPSi) and THCPSi (Thermal hydrocarbonization of PSi)	Peptide YY3−36 (PYY3-36)	30.4, 48.5 and 47.1, respectively	163, 180 and 157, respectively	15.3, 12.3 and 11.8, respectively	−47.8, −40.5 and −31.4, respectively	PSi nanocarriers improved sc PYY3-36 delivery, showing sustained release and enhanced bioavailability regarding IV delivery. More hydrophobic PSi surface resulted in more sustained PYY3-36 release *in vivo*.	[65]
Intramuscular, subcutaneous and intravenous	MSN-SS(disulfide bound)-MXF	Moxifloxacin (MXF)	35.9	182	–	−30	MSN-SS-MTX comprises an interesting nanoplatform for model of pulmonary tularemia, which was more effective than free MTX. The intramuscular route was more effective than the intravenous route for this treatment.	[66]
Intratumoral	pH-responsive biodegradable hollow mesoporous organosilica nanoparticles (PBHMONs)	DOX	86.4	~100	2.2	–	The nanoplatform entered the tumor cells via EPR. The weakly acidic microenvironment induced the biodegradation of the PBHMONs, leading to partial drug release upon degradation of the carrier and efficient cancer cell killing, as well as rapid excretion.	[67]
Intratumoral	Gem-PFH-Au star(gold nanostar)-HMS-IGF1 (insulin-like growth factor-1)	Gemcitabine (Gem) and perfluorohexane (PFH)	95.2 and 0.94, respectively	~200	–	–	Excellent nanoplatform for multimodal US (ultrasound)/CT/PA/thermography imaging-guided interventional therapy for pancreatic cancer.	[68]
Intratumoral	Au@MPPD(mesoporous silica nanoparticles modified with triphenylphosphine and loaded with DOX)@HA	DOX and HA	20.8	45	2.5	~ +15	Au@MPPD@HA was highly cytotoxic to cancer cells but biofriendly to normal tissues. Under NIR light, PTT effectively suppressed tumor growth, and associated with DOX release, a synergistic effect was detected, suggesting the nanosystem for chemophototherapeutic cancer treatment.	[69]
Intratumoral	PRN@MSN	Propranolol (PRN)	–	125	2.6	−5.03	This nanoplatform induced autophagy dysfunction with excessive autophagosome accumulation to promote the therapeutic efficacy of PRN against infantile hemangioma.	[70]
Intratumoral	HMSN-NH_2-TPT-CGO(carboxylated Graphene oxide)	Topotecan (TPT)	~ 68	~ 190.3	~ 24.5	−15.8	Nanocarriers exhibited effective and enhanced *in vitro* and *in vivo* apoptosis, as well as significant tumor growth inhibition, even after 15 days of treatment time, with no toxic effect on the vital organs.	[71]
Intratumoral	DOX-CuS@PMOs (periodic mesoporous organosilica nanoparticles)	DOX	94	299	2.67	74.2	Mild hyperthermia induced by laser-irradiated CuS nanoparticles improved cell uptake of nanotheranostics both *in vitro* and *in vivo*, enhancing the chemotherapeutic efficacy for complete tumor growth suppression without recurrence.	[72]
Intratumoral	UCNP(upconversion nanoparticles)@SiO_2@$mSiO_2$ (mesoporous silica)-SP (spiropyran)-CUR	CUR	18.5	100	2.9	–	CUR can be "uncaged" via NIR irradiation-triggered hydrophobicity-hydrophilicity switch of the spiropyran, inducing drug release and recovering their bioactivity. Under NIR light, the UV/Visible emissions from UCNP can initiate the generation of reactive oxygen species (ROS) by Cur, improving therapeutic efficiency.	[73]
Intratumoral	MSN-SP(sodium phthalate salt)-LPS (lipopolysaccharide)-DOX	DOX	–	~ 167.1	~ 2	~ −11	MSN-SP-LPS pathogen-mimicries elicited high production of ROS in tumor microenvironment; excessive production of	[74]

(*continued on next page*)

Table 1 (*continued*)

Administration routes	Carriers/composition	Drugs	Encapsulation efficiency (%)	Particle size (nm)	Pore size (nm)	Zeta potential (mV)	Main results/goal	Reference
							ROS in turn oxidized the arylboronic ester to perform controlled chemotherapy; the nanocomplex self-stimulated macrophages activation, activating cytotoxic T cells for an anti-tumor immune response. Chemotherapy and immunotherapy acted synergisticallyto inhibit solid tumor growth.	
Ophthalmic	BEV@ MSN-PEG-NH_2	Bevacizumab (BEV)	79.2	140	9.8	6.9	BEV@ MSN-PEG-NH_2 nanosystem improved BEV angiogenic effect *in vitro* and *in vivo*.	[24]
Ophthalmic	BMD-AMS (amino-functionalized mesoporous silica nanoparticles)	Brimonidine (BMD)	4.17	1000–3000	3.8	−41.8	The AMS particles were adhesive to the mucous layer lining the eye surface to allow a high preocular retention property. In addition, AMS remained in the preocular space longer and concurrently released the drug in a sustained manner, enhancing ocular drug bioavailability.	[75]
Nasal	Curcumin loaded MSNP (CUR-MSNP) and chyrsin loaded MSNP (CHRY-MSNP)	Curcumin (CUR) and chrysin (CHRY)	12.3 for both	200–283	1.93	−23.9–16.9	Promising characteristics of MSNs for nose-to-brain delivery	[76]
Nasal	MSNs coated with polylactic acid (PLA) and modified with LDLR ligand peptide (LPMSNPs)	Resveratrol (RSV)	1.6	200	4.0	–	The conjugation of LDLR ligand peptide to MSNs promoted a reduction in microglia infammation and superoxide production.	[77]
Nasal	BSeC@MSNs-RGD ((arginine–glycine–aspartate) peptide)	Organic selenium compound (BSeC)	12	136	–	+29.6	MSNs-RGD enhanced the cellular uptake of BSeC by recognition of RGD peptide on glioblastoma cells which overexpress integrins, besides its ability to inhibit the tumor spheroid growth in tumor model *in vitro*.	[78]
Nasal	MSNs@DOX conjugated with PEI-cRGD (polyetherimide-cricoids Arg-Gly-Asp-Phe-Lys) peptide	DOX	7.65–10.57	20–80	2.6–3.3	~ −15-+45	DOX@MSNs functionalized with PEI-cRGD showed greater selectivity and antitumor activity in glioblastoma cells. Besides, the MSNs with smaller diameter increased the permeability across the BBB.	[79]
Nasal	ANG(modified Angiopep-2 peptide)-PTX-PLGA (modified poly(lactic-co-glycolic acid))-DOX-MSNs)	DOX and paclitaxel (PTX)	77 - 90 and 85–93, respectively	~ 30-60	–	−20–36	Functionalization with Angiopep-2 resulted in higher cytotoxicity, cell uptake and BBB permeability due to selectivity of the peptide at the LRP receptor.	[80]
Nasal	MSNP-TMZ-coated with PDA(polydopamine)-NGR (modified with Asn-Gly-Arg)	Temozolomide (TMZ)	25.6	62–129	–	−40 -+21	The modification of NGR ligand to MSNs nanocarriers was beneficial: it enhanced the antitumor effect of drugs associated with autophagy inhibition mediated by 3-MA.	[81]
Nasal	H_2O_2-responsive MSNs functionalized with 3-carboxyphenylboronic acid and coated with immunoglobulin G (IgG)	Metal chelator clioquinol (CQ)	–	100	–	–	MSNs showed promising properties in terms of Aβ aggregation inhibition, neurotoxic ROS reduction, and high cell viability on rat pheochromocytoma PC12 cells.	[82]
Nasal	H_2O_2-responsive MSNs-CQ-AuNPs (gold nanoparticles)	Metal chelator clioquinol (CQ)	–	~ 50	2.57	+20.6–26.7	*In vitro* co-culture model of BBB confirmed the high ability of MSNs to cross the BBB, the intracellular release of CQ, besides Aβ aggregation inhibition mediated by gold nanoparticles.	[83]
Pulmonary	MSNs combined with two types of siRNA targeted to MRP1 and BCL2 messenger RNA (mRNA), and modified with LHRH peptide	DOX and cisplatin (CIS)	8 and 30, respectively	180	2.8	–	The combination of siRNAs promoted higher cytotoxicity for both drugs in human lung cancer cells, and higher accumulation of MSNs into mouse lungs, confirming its potential for inhalation delivery.	[84]
Pulmonary		–	–	70	2	–		[85]

(*continued on next page*)

Table 1 (*continued*)

Administration routes	Carriers/composition	Drugs	Encapsulation efficiency (%)	Particle size (nm)	Pore size (nm)	Zeta potential (mV)	Main results/goal	Reference
	MSNs coated with polyethyleneimine (PEI), and functionalized with fluorescein isothiocyanate (FITC)						MSNs has the ability to achieve bronchial tree and lung macrophages, confirming its potential for drug delivery into the respiratory tract.	
Dermal	Q/copoly(copolymerization of N-isopropylacrylamide (NIPAM) and 3-(methacryloxypropyl) trimethoxysilane (MPS))-MSN_{small} and Q/copoly-MSN_{big}	Quercetin (Q)	26.4–39.4	200 and 328, respecitvely	~ 3.5 and 5, respectively	−20.6 and −21.3, respectively	Q/copoly-MSNbig exhibited more evident thermoresponsive behavior, proving the potential of these thermosensitive systems for advanced dermal delivery.	[86]
Dermal	MTX/MSN	MTX	37.8–39.4	200	–	−16.1	MTX-loaded MSN was capable of delivering the drug to the deeper layers of the epidermis. Drug skin absorption was significantly enhanced by the addition of shea butter, found to act as a penetration enhancer whose effectiveness depended on the kind of vegetable oil used.	[87]
Dermal	5-ALA@HMSNP-PEG + FA	5-Aminolevulinic acid (5-ALA)	3.4	150	2.1–2.7	–	Cellular uptake of 5-ALA and PphIX accumulation were significantly enhanced by using 5-5-ALA@HMSNP-PEG + FA. Upon red light irradiation for PDT, efficient cancer cell killing effect from 5-ALA@HMSNP-PEG + FA was demonstrated, rendering it a promising nanosystem for skin cancer treatment.	[88]
Dermal	MSNPs-MB-PLL(poly-L-lysine)	MB (molecular beacon, a model of oligonucleotide)	1.42	200–250	4	+30	From topical delivery of siRNA with MSNPs for skin tumor treatment, the release rates of siRNA were the same as those of MBs, and TGFβR-1 gene expression in RT3 cells was reduced by 60% relative to the control. MSNSPs-MB-PLL are interesting nanosystems for topical formulation to treat skin squamous cell carcinoma (SCC).	[89]
Dermal	LIDO/MCM41(MSNs)-NH_2 (APTES)	Lidocaine (LIDO)	79.9–99.7	45–95	0.23–2.61	+23- + 33	From *ex vivo* skin permeation, LIDO/MCM41-NH_2 enhanced LIDO permeation, with 64% of LIDO content released in 24 h, while LIDO release was 13% from the bare MSNs.	[90]
Dermal	DA(N-[3-(trimethoxysilyl)- propyl]ethylenediamine) MSN, ZnDAMSN, periodic mesoporous organosilica nanoparticles containing bridging ethane (PMOBTE) and periodic mesoporous organosilica nanoparticles containing bridging benzene (PMOBTB)	N-[3-(trimethoxysilyl)- propyl] ethylenediamine (DA), Zn^{2+} ions, ethane and benzene bridges	–	179–357	2.8–13.6	–	Promising characteristics of MSN, with their potential for sunscreen applications.	[91]
Dermal	2-Ethylhexyl salicylate was physically encapsulated in hollow silica nanoparticles (E-Sal), particles were coated with an additional shell or cap of silica (cap-E-Sal), salicylate attached to the silica matrix through single (P-Sal) or two silsesquioxane groups (B-Sal) and particles based on curcuminoid-bridged monomer (B-Curc)	Salicylate and curcumeroid sunscreens	0.85–2.88	657–809	2–3.1	–	Hollow silica nanoparticles were prepared and both the salicylate and curcuminoid particles could be classified as broad-spectrum, and they ranged from moderate to superior in terms of UVA protective ability.	[92]
Dermal	MSN-CAF and MSN-RUT	Caffeic acid (CAF) or rutin (RUT)	–	220–223	3	−19.5 and −22, respectively	RUT yielded the best results in terms of antioxidant capacity preservation during coupling procedures, cellular toxicity alleviation, and decrease in ROS level after 24 h incubation of cells with grafted nanoparticles. The coupling of RUT to silica nanoparticles was beneficial in terms of ROS reduction, cellular viability, and protective	[93]

(*continued on next page*)

Table 1 (*continued*)

Administration routes	Carriers/composition	Drugs	Encapsulation efficiency (%)	Particle size (nm)	Pore size (nm)	Zeta potential (mV)	Main results/goal	Reference
							effects mediated through the activation of the Nrf2 antioxidant pathway.	
Dermal		Chlorhexidine		53–477	2.86–2.88		Spherical nanoparticle-encapsulated CHX could preferably enhance its antibiofilm efficiency through an effective releasing mode and close interactions with microbes.	[94]
Dermal	(THPMA-co-AEMA)-g((tetrahydropyranyl methacrylate-co-amino ethyl methacrylate)-grafted)-MSN	5-flurouracil (5-FU)	–	104.9–137.2	3.73–3.8	+31.3 – +32.7	*In vivo* Chorioallantoic membrane (CAM) assay confirmed that the fabricated material could prevent premature drug leakage in addition to its capability of sustained release and anti-angiogenesis activity.	[95]
Oral	IMC-MSNRs (mesoporous silica nanorods) and IMC-MSNSs	Indomethacin (IMC)	~ 29 and 22, respectively	–	5.8 and 4.7, respectively	–	IMC-MSNRs and IMC-MSNSs showed low drug loading but excellent dissolution- enhancing effect (100% of IMC release after 1 h), being important nanosystems to overcome poor aqueous solubility of IMC.	[96]
Oral	MSM (mesoporous microparticles)-A-CUR and MSN-A (amine functionalized)-CUR	CUR	–	1000 and 100, respectively	10	–	The nanosystems improved *in vitro* solubility of CUR and the bioavailability in mice after oral administration.	[97]
Oral	H(hollow)MSMs-CUR	CUR	47.8	725	~ 2.5	–	Good *in vitro* release behavior of CUR from HMSMs@CUR An impressive improvement in the *in vivo* oral absorption and prolonged systemic circulation time were achieved. Non-cytotoxicity was observed for HMSMs with Caco-2 cells.	[98]
Oral	MSNs-TEL	Telmisartan (TEL)	–	20–90	–	–	MSNs significantly enhanced TEL permeability and reduced the rate of P-gp mediated drug efflux. Enhanced *in vivo* pharmacokinetics was demonstrated for the MSN-TEL formulation when compared with a commercial formulation.	[99]
Oral	MSN-CTB	Cholera toxin subunit B (CTB)	–	300–350	8	–	The superior immune response in the MSN-CTB-immunized group suggested that compared to MCN (mesoporous carbon nanoparticles), MSN was a better choice for protection, delivery, and release of antigen against *V. cholerae* in an oral vaccine formulation.	[100]
Oral	Spherical-shaped MSNs with AR = 1 (NSs), short-rod MSNs with AR = 1.75 (NSRs) and long-rod MSNs with AR = 5 (NLRs)	–	–	83, 83 width and 146 length, 96 width and 483 length	–	−20–−25	With the decrease of AR, the systematic absorption by the small intestine and other organs increased and the urinary excretion decreased. The biodistribution tendency was consistent with the MSNs degradation rate in simulated body and intestinal fluid. Particle shape-dependent renal toxicity of MSNs was observed.	[101]
Oral	MSN-PMV(Poly (methacrylic acid-co-vinyl triethoxylsilane))-INS	Insulin (INS)	39	–	65	–	pH responsive behavior of PMV helped in monitoring INS release, more pronounced in intestinal region. Pharmacodynamic and pharmacokinetic response of orally administered MSN-PMV-INS displayed	[102]

(*continued on next page*)

Table 1 (*continued*)

Administration routes	Carriers/composition	Drugs	Encapsulation efficiency (%)	Particle size (nm)	Pore size (nm)	Zeta potential (mV)	Main results/goal	Reference
							potential of this novel formulation for oral INS delivery.	
Oral	L-(lipid-coated)MSNs@CIP	Ciprofloxacin (CIP)	–	50–100	–	–	L-MSN@CIP showed improved antibacterial activity in clearing intravacuolar *Salmonella* infection. The L-MSN particle system exhibited controlled release of CIP. The lipid coat around the particle improved its biocompatibility and aided in intravacuolar targeting of the drug cargo, leading to a lower requirement of CIP dose as detected in the *in vivo* model.	[103]
Oral	MSNs with molecular level chiral function property (F-MSNs), namely levorotatory MSNs (FL-MSNs) and dextrorotatory MSNs (FD-MSNs)	Nimesulide (NMS)	–	200–300	2.71–2.74	–	*In vivo* pharmacokinetic and anti-inflammatory pharmacodynamic studies indicated that FL-MSNs and FD-MSNs improved the oral bioavailability of NMS (698.45 and 887.03%, respectively), and FD-MSNs delivered more NMS after responding to the *in vivo* environment, presenting stronger anti-inflammatory pharmacodynamic effect.	[104]

nanocarriers to treat organs and diseases. The main administration routes that exploit the remarkable properties of MSNs comprise intravenous, subcutaneous, intramuscular, intratumoral, ophthalmic, pulmonary, nasal, dermal, and oral routes. Table 1 depicts these routes for MSNs as drug carriers, types of efficient MSNs-based nanoplatforms, their physicochemical parameters, and main results.

3.1. Intravenous route for MSNs administration

The intravenous (IV) injection is the fastest invasive administration route allowing good drug delivery control, high bioavailability even at low doses, and immediate response. By using IV injection, the estimated time from the bloodstream to the brain is between 20 and 40 s. The IV route is suitable for drugs that cannot be absorbed in the gastrointestinal tract or hardly applied via subcutaneous (SC) or intramuscular (IM) routes [105–107]. However, some drawbacks of IV routes include pain for the patient, high cost, resistance by the first-pass effect on the liver, easy contamination, and the requirement of experienced healthcare personnel and tools for the method to be safe [2,105,106]. To overcome these limitations, the design of multifunctional MSNs as specific drug delivery nanoplatforms is essential to improve the administration route advantages and minimize the reported side effects [2,4,38].

Balasubramanian et al. [27] designed modified porous silicon nanoparticles (UnPSi NPs) covalently conjugated with a specific antibody (anti-PSA-NCAM) against polysialylated neural cell adhesion molecule (PSA-NCAM). The nanoplatform was loaded with SC-79 drug to increase the Akt signaling pathway in doublecortin positive neuroblasts. The engineered nanosystems were successfully fabricated and characterized. Cytotoxicity assays in cultures of primary embryonic neuronal stem/progenitor cells (NSPCs) at different anti-PSA-NCAM-UnPSi NPs concentrations were performed, and no significant cytotoxicity was detected, suggesting good cytocompatibility. In addition, the authors reported a concentration-dependent cellular uptake caused by these nanosystems. *In vivo* targeting assays were carried out by intravenous injection of iodine-125 -radiolabeled anti-PSA-NCAM-PE-UnPSi NPs in a rat model of stroke. By the IV administration route, 125I-labeled anti-PSA-NCAM-PE-UnPSi NPs displayed maximum signal in the brain at 2 h post-injection, but with prominent accumulation in the liver and spleen, suggesting that IV nanosystem injection was feasible. In the evaluation of targeting properties, aiming to reduce and avoid immune recognition and reticulo-endothelial system (RES) clearance, local bilateral intraventricular injections were performed. Furthermore, the authors exhibited the real potential of targeted delivery of SC-79 by anti-PSA-NCAM-PE-UnPSi NPs to stimulate the Akt pathway in endogenous doublecortin (DCX^{+}) neuroblasts in the subventricular zone (SVZ). This multifunctional nanoplatform comprises a novel tool to develop new therapeutic strategies aiming at regenerating functional neurocircuitry after stroke.

Chen et al. [39] prepared a multifunctional MSNs nanodrug (Ru-MSN-PLip) by loading RuDPNI complex into MSNs pores (Ru-MSN) covered with a protein-incorporated liposome (PLip) to achieve multiple targeting and eGFP-based fluorescence imaging of non-small cell lung cancer. All synthesis steps were successfully performed and the nanosystems were well characterized. The Ru-MSN-PLip nanosystem was stable and hardly precipitated under physiological conditions. From *in vitro* tests, specific and high cellular uptake was detected for Ru-MSN-PLip in H1299 tumor cells, compared with other cells and precursor nanosystems. By nanosystem IV administration, *in vivo* assays exhibited RuMSN-PLip long-term blood circulation, biocompatibility, accumulation in tumors, and consequently tumor growth inhibition. The authors' findings [39] shed light on the potential applications of bioreducible and traceable nanoprodrugs for efficient and safe non-small cell lung cancer therapy. These results suggest that these nanoprodrugs can be used as theranostic platforms for efficient and safe non-small cell lung cancer treatment.

Li et al. [40] reported the fabrication of multi-responsive and biodegradable theranostic nanoplatforms based on hollow mesoporous organosilica nanoparticles (HMONs) for highly efficient photoacoustic (PA) imaging-guided chemo-photothermal therapy (PTT) of human osteosarcoma cancer. HMONs were impregnated with DOX and then decorated with biocompatible nanocomposites (CuS@BSA) through a GSH-sensitive disulfide bond (labeled as CuS@BSA-HMONs-DOX). The theranostic nanosystems exhibited GSH-responsive breakage in the tumor microenvironment of the disulfide bonds in the HMONs structure and the linker between HMONs and BSA, leading to the DOX release and tumor-specific biodegradation. Besides, the nanosystems were also acid pH and mild hyperthermia-responsive, promoting DOX release. CuS@BSA-HMONs-DOX presented strong absorbance in near-infrared (NIR) region, leading to excellent diagnostic performance on the PA imaging modalities. The CuS exhibited high photothermal conversion efficiency (51.5%) for hyperthermia. These results configured CuS@BSA-HMONs-DOX as a pH-, NIR- and GSH-sensitive nanoplatform for DOX release, performing synergistic chemo-phototherapy functions. From *in vitro* and *in vivo* assays, effective DOX delivery to tumor sites/cancer cells and induced mild hyperthermia were detected, resulting in enhanced suppression of tumor growth after synergistic chemo-photothermal treatment. In addition, by IV nanoplatform administration, the high nanosystem concentration in the tumor was observed at 12 h, while most nanosystems are detected in RES organs (liver and spleen) at 24 h. The pH/GSH/NIR tri-stimuli-responsive CuS@BSA-HMONs-DOX nanoplatform, combined with excellent biocompatibility and biodegradability, comprises an excellent and innovative nanotheranostic tool for imaging-guided and synergistic treatments.

In another study [60], the researchers designed an intelligent biomimetic theranostic nanoplatform by integrating inflammation-activatable neutrophils with core-shell structured magnetic mesoporous silica nanoparticles (MMSNs) containing DOX (labeled ND-MMSNs) to treat remaining glioma after surgical resection of primary tumors. ND-MMSNs were prepared by internalizing Dox-loaded MMSNs into neutrophils, which still maintained cellular activity and could actively target the inflamed glioma site for therapeutic purposes. In addition, the phagocytic MMSNs possessed cell tracking capability (magnetic resonance imaging [MRI] tracking), providing a diagnosis of residual tumor and therapeutic guidance. Furthermore, improved survival rate and delayed glioma relapse were demonstrated in surgically treated glioma mouse models after IV administration of ND-MMSNs, showing that neutrophils carrying D-MMSNs could effectively identify the inflammatory signals derived from surgical management and accumulate in the remaining tumor site to maximize the drug bioavailability. This strategy provides a new insight to track the fate of neutrophils by MRI and explore immune cell-based drug delivery systems (CDDSs) to treat diseases associated with inflammation.

3.2. Subcutaneous route for MSNs administration

The subcutaneous (SC) administration route is an interesting alternative to IV administration by which carriers and drugs can be delivered without using blood vessels as injection sites, reducing fast clearance processes and optimizing therapeutic effects. Besides, the SC administration route is widely used to deliver systems with poor oral bioavailability, showing advantages such as good acceptance by patients, higher safety, effectiveness, and reduced healthcare costs in comparison with IV injection. Drug delivery systems can usually be transported from the injection site to lymph nodes according to the lymphatic flow rates and carrier physicochemical properties. The carrier size parameter is essential to assess whether the delivery platforms will remain in injection sites or will be absorbed for the lymphatic system. The authors reported that carriers with few nanometers in size can be drained, thus reaching the lymphatic system, whereas larger carriers remain longer at the application site [2,108,109].

Kovalainen et al. [65] reported the fabrication of three nanoplatforms based on mesoporous silicon nanoparticles (PSi), thermally oxidized (TOPSi, hydrophilic), undecylenic acid-treated thermally hydrocarbonized (UnTHCPSi, moderately hydrophilic), and thermally hydrocarbonized (THCPSi, hydrophobic). These nanocarriers were evaluated for sustained SC and IV peptide YY3−36 (PYY3-36) delivery. The authors showed that the evaluated administration routes directly influenced PYY3-36 release from the nanoplatforms *in vivo*. The investigated PSi nanocarriers improved SC PYY3-36 delivery, showing sustained release (over 4 days) and enhanced bioavailability in comparison with the IV administration route. The hydrophobicity of the PSi nanocarrier (THCPSi) decreased the *in vivo* release rate of PYY3-36, indicating that peptide release can be modified by changing the PSi surface chemistry. The authors demonstrated that IV administration of nanocarriers did not sustain PYY3-36 delivery, suggesting their rapid clearance from the bloodstream circulation to the liver and spleen. These results exhibited the feasibility of PSi nanocarriers for the sustained PYY3-36 delivery via the SC administration route.

Nguyen et al. [62] fabricated an injectable dual-scale mesoporous silica vaccine (MSR-MSN) consisting of MSNs loaded with Ovalbumin (OVA) and CpG oligodeoxynucleotides (CpG-ODNs) combined with mesoporous silica microrods (MSRs) loaded with dendritic cells (DC)-recruiting chemokine (granulocyte-macrophage colony-stimulating factor, GM-CSF) for cancer immunotherapy. MSRs formed a three-dimensional macroporous scaffold after SC injection, and the subsequent release of DC-recruiting chemokine loaded in the mesopores of MSRs led to the recruitment of numerous DCs into the scaffold. Subsequently, MSNs co-loaded with an OVA antigen and CpG-ODNs were internalized by the recruited DCs, leading to the generation of antigen-presenting activated DCs. The MSR-MSN dual-scale vaccine generated a significantly larger number of antigen-specific T cells displaying higher B16-OVA melanoma suppression than single MSR or MSN vaccines. In addition, the dual-scale vaccine was synergized with the immune checkpoint anti-cytotoxic T-lymphocyte-associated antigen 4 antibody (a-CTLA-4) to treat tumor-bearing mice and enhance their survival rate. These findings indicated that MSR-MSN acts as a dual-mesoporous silica vaccine for further enhancement of cancer immunotherapy.

Wang et al. [63] constructed a core-shell two-step precise targeting nanoplatform based on MSNs modified with triphenylphosphonium (TPP) and loaded with 2,2′-azobis[2-(2-imidazolin-2-yl) propane] dihydrochloride (AIPH) covered with pH-sensitive liposomes containing docetaxel and modified with folic acid as a target agent (Lipo/DTX-FA). These nanosystems were characterized, and *in vitro* tests exhibited high specificity tumor cell uptake through FA receptor-mediated endocytosis. The pH-sensitive liposomes were destabilized in the lysosomes, resulting in DTX release and AIPH/MSN-TPP nanoparticles. TPP-modified nanosystems acted as mitochondria targeting, promoting the AIPH delivery and then, the production of alkyl radicals under the high-temperature environment, causing oxidative damage to the organelle. Additionally, DTX was able to enhance the anti-tumor effect of AIPH by down-regulating the expression of antiapoptotic Bcl-2 protein. From *in vivo* assays, via SC administration, the targeting nanosystems accumulated more effectively in the tumor site and showed longer *in vivo* retention time than the non-targeted group. These results demonstrated the preparation of a precise dual-targeted nanoplatform as a new approach to chemotherapy.

3.3. Intramuscular route for MSNs administration

The intramuscular (IM) administration involves injection into the high vascularity of muscle tissue to achieve a moderately rapid onset of action, usually within 5–10 min, faster than that of the SC injection. IM injections are used when effects are desired over a longer period than can be expected after IV injection, for drugs that are too irritant to be given subcutaneously, or for oily solutions, which cannot be given intravenously [107,110]. When the drug is adequately administered, its

absorption from an IM injection deep into a large muscle is much faster and more dependable than that given by the oral route. The absorption rates vary as a function of solution/suspension physiochemical properties and physiological variables such as muscle blood circulation and the state of muscular activity [111]. Besides, the IM route is the most feasible injection route because it requires no special equipment (only a syringe and needle) or patient cooperation [107,110]. However, it has the disadvantage that the IM route limits the amount injected to the muscle mass available and, like all injection routes, it causes pain at the injection site [111]. To date, few results concerning the IM route for MSNs administration have been reported [66,112].

Interestingly, Clemens et al. [66] evaluated the action of free moxifloxacin (MXF) and disulfide snap-top redox-operated MSNs containing MXF (MSN-SS-MXF) to treat pneumonic tularemia via three distinct administration routes: intravenous (IV), subcutaneous (SC), and intramuscular (IM) routes. From preclinical assays using equivalent amounts of MXF, the highest efficacy to treat pneumonic tularemia was achieved by IM MSN-SS-MXF followed by SC MSN-SS-MXF and IV MSN-SS-MXF. In addition, the targeted nanoplatform was more effective than free MXF, for all administration routes. Despite the targeting ability of modified-MSNs to reach infected cells or tissues, the greatest efficacy of this nanoplatform was ascribed to the markedly longer half-life of MXF and the markedly longer duration of MXF blood levels above the minimal inhibitory concentration (MIC). These results can be attributed to the pharmacokinetic enhancement achieved by using MSN-SS-MXF via the IM administration route, in comparison with other evaluated routes.

3.4. Intratumoral route for MSNs administration

Similarly to SC administration, the intratumoral (IT) administration route is performed in specific sites, in this case, tumor tissues. Nowadays, the IT route is extensively applied in animal models (preclinical assays), showing promising and interesting potential for clinical applications. This administration route can overcome drawbacks, such as systemic administration, and the targeting nanoplatforms can be designed considering the direct application into the interstitium of cancer cells/tissues [2,113]. Therefore, factors such as the acid pH of tumor cells, absence of vascularization in tumor tissues, and higher interstitial pressure in tumor tissues than in healthy tissues, can provoke higher leakage of the administered nanosystems to the surrounding healthy tissues. In addition, the IT administration route is currently considered only for accessible and external tumor tissues [2,113]. As mentioned above for the SC route, factors such as surface and particle size also influence the biodistribution and clearance of the nanosystems.

Zhou et al. [69] prepared a nanocomposite hydrogel containing triphenylphosphine (TPP) modified core-shell gold MSNs loaded with DOX and covalently embedded with hyaluronic acid (HA) as a targeting drug delivery system for sustained stomach cancer treatment. HA constitutes the extracellular matrix and shows an affinity for the CD44-overexpressed cancer cell. As mentioned above, TPP acts as a targeting agent for mitochondria. The Au@MPPD@HA exhibited high specificity and toxicity for cancer cells whereas the nanocomposites were biofriendly to healthy cells. After IT injection, the Au@MPPD@HA released, in a controlled manner, the Au@MPPD nanosystems by the action of tumor-specific exocrine HAase degrading HA hydrogel. The nanosystems released selectively attacked cancer cells and then the mitochondria, thus exhibiting good multistage-targeted properties. Additionally, the Au@MPPD nanosystem (via core Au nanoparticles) converted NIR light irradiation into thermal energy, inducing tumor growth suppression, and showed a synergistic therapeutic effect associated with DOX. These nanocomposites displayed an excellent chemophotothermal effect on a gastric tumor comprising a multistage-target drug-delivery nanoplatform for synergistic cancer chemophototherapy.

Liu et al. [73] synthesized upconversion nanoparticles (Yb/Tm co-doped NaYF4, UCNP) coated with spiropyran (SP)-modified mesoporous silica ($mSiO_2$) and loaded with curcumin (CUR) as a NIR-controlled cage-mimicking system for hydrophobic drug-mediated cancer therapy. The authors reported that CUR stability increased and drug release was efficiently controlled by the hydrophobic layer composed of SP. Under NIR light irradiation, UCNP absorbed this light and converted it into ultraviolet/visible (UV/Vis) light that allowed the conformational change of SP, opening the blocked mesopores and promoting CUR release and activation. NIR light is suitable for *in vivo* studies due to its deep tissue penetration and ability to generate UV–Vis light, which sensitized CUR promoting reactive oxygen species (ROS) production, enhancing the UCNP@$mSiO_2$@CUR-SP therapeutic efficiency. From *in vivo* assays, both IT and IV routes were evaluated. In IT administration, the nanosystem was well-distributed in tumor issues after 4 h or 24 h treatment with minimal spread from the tumor site to other organs. On the other hand, in IV injection, fast and high nanosystem accumulation was detected in the liver and spleen, with little accumulation in the lung, heart, kidney, and tumor. In this sense, IT injection was the most efficient administration route for nanosystem delivery and antitumor efficacy. Additionally, *in vivo* assays displayed the best tumor suppression ability when the photo-controlled drug delivery nanosystems were irradiated with NIR light, suggesting the synergistic chemotherapy and photodynamic therapy.

Dong et al. [74] constructed a DOX-loaded sodium phthalate salt of parent lipopolysaccharide (SP-LPS) coated MSNs (labeled MSN-SP-LPS) as gram-negative bacteria-mimicking nanosystem for synergistic chemoimmunotherapy. The amino-modified MSNs were reacted in a second step with 4-carboxyphenylboronic acid (CBA) subsequently loaded with DOX, and finally, modified with detoxified lipopolysaccharide (SP-LPS). The novel nanoplatform was successfully characterized, proving the MSN-SP-LPS preparation. The modification with SP-LPS exhibited a dual function: it mimicked the pathogen to trigger immune responses and avoided premature DOX release from the nanoplatform. The developed nanosystem was recognized similarly to the pathogenic agent, and it promoted the enhancement of ROS production at the site tumor environment. The arylboronic ester in the nanosystem was ROS-sensitive, so the ROS enhancement in the tumor site led to its oxidation, opening the blocked mesopores and promoting controlled DOX release. In addition, the nanosystems displayed the ability to self-stimulate macrophages activation, which subsequently activated T cells for an anti-tumor immune response. *In vivo* assays were performed to corroborate *in vitro* results, before further clinical trials. By the IT injection route, the MSN-SP-LPS were nontoxic and did not induce systemic inflammation to healthy tissues. The nanoplatform biodistribution was evaluated, and within 7 days, 24% was observed in tumors whereas the liver retained the highest amount and the kidney a small amount, suggesting that the main clearance occurred via hepatobiliary excretion. The DOX-controlled release was confirmed by the opening of the ROS-sensitive mesoporous blockers and the immune activity was demonstrated by the higher tumor necrosis factor-alpha (TNF-α) concentration achieved by using MSN-SP-LPS, subsequently stimulating T cells and then anti-cancer immune response. All results confirmed high nanoplatform performance for synergistic chemoimmunotherapy in preclinical assays, suggesting them as novel nanotools for further clinical tests.

3.5. Ophthalmic route for MSNs administration

Ocular drug delivery and absorption pose a big challenge due to the unique characteristics of the eye anatomy and physiology. The eye anatomy can be divided into two segments: the anterior segment, which consists of the cornea, iris, lens, and aqueous humor, and the posterior segment, which includes the vitreous body, retina, choroid, and the back of the sclera [114,115]. There are two main obstacles to achieving high ocular bioavailability, and consequently, high drug absorption: the blood-aqueous barrier (BAB) composed of the inner ciliary epithelia, endothelia around the iris, and ciliary muscle capillaries; and the

blood-retinal barrier (BRB), formed by the endothelia of the retinal capillaries and retinal pigment epithelium [114,115]. Both barriers can be overcome by multifunctional nanoplatforms such as modified drug-loaded MSNs, which enhance drug bioavailability and absorption at the target site. Fig. 2 summarizes the eye anatomy and physiology, showing the barriers to drug absorption and the main possibilities of ophthalmic administration routes.

The choice of ophthalmic administration routes to exploit inorganic systems, especially MSNs as drug carriers, has so far been limited. In this sense, Sun et al. [24] reported the fabrication of amino-modified MSNs-encapsulated bevacizumab (BEV) nanoplatforms aiming to improve BEV antiangiogenic response and therapy. The nanoplatform (BEV@MSN-PEG-NH_2) was prepared by amino and subsequent PEG-modification and, finally, encapsulation of BEV. The nanosystem was characterized by physicochemical analysis, showing high encapsulation efficiency (EE, 79.2%) and sustained *in vitro* BEV release, with 5% of BEV released in the first 2 days, but with a burst release in the first 1–10 h. About 35% of BEV was released in the next 5 days with subsequent slow release up to 28 days. Additionally, BEV-loaded MSNs did not show any cytotoxic effects on endothelial cell viability at reasonable concentrations (above 1 mg mL^{-1}), suggesting that the BEV angiogenic effect was preserved and improved by using BEV@MSN-PEG-NH_2. *In vivo* assays were performed based on the retinal neovascularization induction in mice. The animals were subjected to intravitreal systems and nanoplatform injections. The author demonstrated that only BEV@-MSN-PEG-NH_2 induced a significant reduction in retinal neovascularization, indicating that inhibition of oxygen-induced retinal angiogenesis is an excellent and promising nanoplatform for anti-angiogenic therapy.

Kim et al. [75] proposed the preparation of amino-functionalized mesoporous silica (AMS) particles containing brimonidine (BMD) as topical delivery carriers to treat glaucoma. The nanosystems were characterized and *in vitro* mucoadhesive tests were performed to assess their mucoadhesiveness to the mucin. The authors reported good mucoadhesive properties ascribed to the presence of both hydroxyl and amino groups onto the nanosystem surface, favoring hydrogen bonds and an ionic complex with the mucin, respectively. From cytotoxic tests, BMD-AMS was found to be nontoxic to L929 mouse fibroblast cells (KCLB) and human primary corneal epithelial cells (HCECs). *In vitro* release studies showed sustained BMD release over 8 h resulting from the out-diffusion of BMD encapsulated into nanoscale mesopores. *In vivo* assays were carried out by topical administration of BMD-AMS suspension to rabbit eyes. *In vivo* mucoadhesive results showed that BMD-AMS remained onto the preocular surface for 1 h, and more than 20% was found after 4 h, which slowly disappeared over the next 12 h, suggesting that BMD-AMS was adhering to the mucous layer at the preocular surface. In addition, the variance in intraocular pressure (IOP) and BMD concentration in the aqueous humor (AH) after applying BMD-AMS to the eye were examined and compared with commercial BMD eye drops. The results of BMD-AMS administration exhibited a decrease in IOP, and the area under the BMD concentration in the AH-time curve (AUC) was 12 h and 2.68 μg h mL^{-1}, respectively, which were about twice as large as the values obtained with commercial BMD eye drops. These findings suggest that this nanoplatform is a promising carrier for enhanced bioavailability of a topically delivered ocular drug.

3.6. Pulmonary route for MSNs administration

The great interest in the pulmonary pathway is related to systemic drug delivery or lung disease therapy. Lung has a large surface area (150 m^2) composed of alveoli and airways, characterized by high vascularization and endothelial permeability, which favor systemic drug delivery and/or localized therapy [2,116]. Lung drug delivery can be performed by the inhalation route. This pathway exhibits advantages such as specific lung drug delivery leading to enhanced drug accumulation and retention at the action site (target cells/tissues), thus reducing systemic side effects. Additionally, this route makes it possible to overcome the limitations of the gastrointestinal tract (GIT) degradation and hepatic metabolism commonly caused by the oral route (Fig. 3) [116].

Efficient lung drug delivery via the inhalation pathway aiming at local or systemic effects depends on lung aerodynamics, particle size, breathing conditions, and inhalation devices [116]. The aerodynamic filter present in the lungs and the mucus lining the pulmonary airways must be overcome in order to favor drug deposition into lung tissue. Between 10 and 40% of the drug is usually deposited into the lungs by an inhalation device [111]. Another lung defensive mechanism that limits inhalation therapy is related to lung macrophages, efflux transporters, and enzymes. It is known that some lung defensive mechanisms can affect systemic therapy more than local therapy by the inhalation pathway [116]. To overcome the drawbacks related to lung deposition, particle size, and specific drug delivery to the respiratory tract and to make lung disease therapy more effective, MSNs have been explored in association with the inhalation route.

Taratula et al. [84] designed multifunctional MSNs by loading doxorubicin (DOX) and cisplatin (CIS), combined with two types of small interfering RNA (siRNA) targeted to MRP1 and BCL2 messenger RNA (mRNA) for suppression of pump and non-pump cellular resistance, and modified with luteinizing hormone-releasing hormone receptor (LHRH) peptide targeted to lung cancer cells. Modified MSNs nanocarriers showed a hexagonal array mesostructure with a pore size of 2.8 nm and particle size of 180 nm, besides values of drug loading of 8 and 30% for DOX and CIS, respectively. The nanosystems combined with two types of siRNA were able to suppress the expression of targeted mRNA (MRP1 and BCL2), resulting in higher cytotoxicity of DOX and CIS in A549 human lung cancer cells, compared to the free drugs. *In vivo* organ distribution assays showed that the MSNs-based nanocarrier inhalation delivery increased the nanosystems accumulation in mouse lungs (73%) significantly, compared to the IV route (5%). Moreover, MSNs-based nanocarriers did not show significant accumulation in other organs (liver, kidneys, or spleen). These findings confirm the potential of MSNs for the treatment of lung cancer by the inhalation route.

In order to achieve the direct delivery of nanocarriers to the respiratory tract, Li et al. [85] engineered MSNs coated with polyethyleneimine (PEI) and functionalized with fluorescein isothiocyanate (FITC, fluorescent dye) as a strategy to evaluate toxicity and MSNs aerosol delivery in pulmonary tissues, using an *in vivo* inhalation model. MSNs nanocarriers with particle diameter and mesopores of 70 and 2 nm, respectively, were obtained. MSNs were aerosolized in respirable-size droplets between 0.1 and 3.0 μm, using a water-based aerosol system for detection in the mouse respiratory tract. Results showed that the aerosolization method did not modify the MSNs structure, remaining stable one week after inhalation. Interestingly, MSNs reached the bronchial tree and gas exchange regions of the mouse pulmonary tract, being able to target these systems to lung macrophages, demonstrating their importance in the treatment of lung infections caused by intracellular pathogens. In addition, no acute pulmonary toxicity was observed during treatment. This work provided a new MSNs delivery strategy to the respiratory system.

Wang et al. [117] reported the development of MSNs with a core (dense silica nanoparticles)-shell structure loaded with paclitaxel (PAC) for lung cancer therapy enhancement. Nanocarriers were obtained with average diameter and pore size of 200 and 5.7 nm, respectively, with a PAC-loaded maximum amount of 45.7%. MSNs significantly increased the PAC release rates, compared to the free drug, showing enhanced absorption by the pulmonary alveoli as determined in rabbit plasma after pulmonary administration. In addition, from MSNs lung biopsy data, inflammation signs were not observed, suggesting their biosafety. PAC-MSNs promoted higher cell apoptosis than free PAC, and cell uptake studies displayed MSNs endocytoses in the cytoplasm by A549 cells. These results suggest that PAC-MSNs are interesting drug delivery nanosystems via the pulmonary administration.

3.7. Nasal route for MSNs administration

The nasal route has been considered an alternative drug administration route to achieve topical and systemic effects. This route emerged as a convenient and safe approach to overcome the limitations of oral and parenteral administrations such as first-pass metabolism and drug degradation/instability in the GIT [111]. Nowadays, the nasal route has been proposed as an effective route for direct drug delivery to the brain aiming to reach the central nervous system (CNS), due to its anatomical characteristics [111,118].

The drug transport mechanism from nose-to-brain involves two main pathways: the intranasal route (olfactory and respiratory regions) and systemic circulation through the blood-brain barrier (BBB) (Fig. 4) [118]. Regarding the nasal cavity region (olfactory and respiratory), differences in cell structure, drug transport mechanism, and drug absorption site were found to play an important role in drug delivery to the brain.

The olfactory region located in the upper portion of the nasal cavity is composed of three major cell types, namely supporting cells, basal cells, and microvillar cells, which are connected by tight junctions. In this region, the drug comes into contact with olfactory and trigeminal neurons, which carry the drug from the olfactory epithelium by intracellular and extracellular mechanisms to the brain. After reaching the brain, the drug is distributed in the CNS via perivascular spaces [118, 119].

The respiratory region is the main area of the nasal cavity, constituted by goblet, basal, ciliated, and non-ciliated cells. This region is highly vascularized with blood vessels and innervated by trigeminal nerves, both responsible for drug transport. The blood vessels favor drug absorption to the systemic circulation whereas trigeminal nerves promote drug entrance to brain pons and cerebrum [118]. Therefore, the olfactory and trigeminal nerves represent a direct connection between the drug and brain, given that nose-to-brain drug delivery can follow one or more pathways.

However, some factors are capable of limiting drug absorption/transport from the nasal route, such as mucociliary clearance, enzymatic activity, and low nasal epithelium permeability, hindering the drug transport to the brain, especially in the CNS [118,120]. To overcome the aforementioned obstacles and enable drug transport through the nasal route, MSNs have been explored due to their high versatility and ease of surface modification with targeting molecules. Additionally, these nanocarriers can favor the transport of molecules over 500 Da and promote the enhancement of drug BBB permeability.

Lungare et al. [76] reported the development of MSNs containing phytochemical drugs (CUR and chrysin [CHRY]) as a strategy for nose-to-brain delivery against CNS diseases. The MSNs loaded with CUR and CHRY were successfully characterized, exhibiting particle size of 200 nm with high surface porosity. *In vitro* release assays revealed a pH-dependent release for both drugs, indicating a greater drug release at the pH of the nasal cavity (5.5). From *in vitro* tests using cultures of olfactory neuroblastoma cells (OBGF400), no significant toxicity was demonstrated for MSNs nanocarriers in both phytochemicals. In addition, the authors associated this behavior with protein corona formed onto the nanosystem surface, leading to alteration of the MSNs cytotoxic potential due to their contact with the serum protein present in the culture media. Besides, MSNs-based nanocarriers with particle size below 500 nm were uptaken by olfactory cells, demonstrating a cytoplasmic accumulation as observed by confocal microscopy. These data exhibited the MSNs feasibility for phytochemical drug delivery to the brain from the nasal administration route.

In another study [77], the researchers proposed to design polylactic acid (PLA)-coated MSNs, conjugated with peptide as a ligand for low-density lipoprotein receptors (LDLR) to achieve targeting delivery of resveratrol (RSV) in the CNS. The authors showed that PLA coating prevented RSV premature release from MSNs-based nanocarriers. The presence of ROS in the release medium promoted the drug release due to PLA degradation. A co-culture of rat brain microvascular endothelial cells (RBECs) and microglia cells were used to assess the RSV delivery across the BBB. Results showed the LDLR ligand peptide-modified MSNs not only promoted an enhancement migration across the RBECs monolayer, but also improved the MSNs-based nanocarrier transcytosis. In addition, RSV was released from the nanocarriers, reducing microglia inflammation and superoxide production, thus indicating a potential application in oxidative stress therapy of the CNS.

You et al. [78] engineered MSNs-based nanocarriers of a novel organic selenium compound BSeC, modified by arginine–glycine–aspartate (RGD) peptide, which recognizes the integrins on tumor membranes to treat brain glioma. The BSeC@MSNs-RGD showed high stability in human blood serum and increased the BBB permeability of BSeC in bEnd.3/U87 co-culture model. In addition, BSeC@MSNs-RGD selectively recognized U87 and bEnd.3 cells, which overexpress integrins, enhancing BSeC cellular uptake. Consequently, BSeC@MSNs-RGD cellular uptake led to mitochondrial dysfunction and intracellular ROS overproduction, inducing cell apoptosis. BSeC@MSNs-RGD also exhibited the ability to inhibit the tumor spheroid growth in a tumor model *in vitro* by using glioblastoma cells U87. These nanosystems prolonged drug blood circulation time *in vivo,* with the drug being cleared by renal excretion, reducing its toxicity, thus comprising an excellent approach to treat human brain glioma.

In another study on glioma therapy, Mo et al. [79] designed MSNs-based nanosystems with tailored size conjugated with PEI-cRGD (polyetherimide-cricoids Arg-Gly-Asp-Phe-Lys) peptide in order to enhance DOX loading efficiency. DOX@MSNs functionalized with PEI-cRGD showed greater selectivity and antitumor activity for U87 glioblastoma cells than the free drug, leading to the cell apoptosis triggered through ROS overproduction. The authors also explained that the smaller the particle diameter (40 nm), the higher the cellular uptake and antitumor activity, since small size hinders particle excretion, resulting in higher drug accumulation. MSNs-based nanocarriers with smaller diameter increased the permeability across the BBB and could interfere with the vasculogenic mimicry capacity of glioma cells due to regulation of FAK, E-cadherin, and MMP-2 protein expression. These nanosystems could achieve interesting antitumor efficacy against glioblastoma.

Heggannavar et al. [80] designed MSNs modified with poly (lactic-co-glycolic acid) (PLGA), loaded with two anticancer drugs (DOX and paclitaxel [PTX]), and later functionalized with Angiopep-2 peptide to achieve targeting for the lipoprotein receptor-related (LRP) protein. LRP is expressed on the blood-brain barrier (BBB) and glioma cells aiming to enhance glioblastoma multiforme treatment efficacy. The authors showed that by controlling the polycondensation degree and hydrolysis rate, different particle sizes were obtained. Functionalization with Angiopep-2 resulted in significant cytotoxicity on U87 cells due to the high selectivity of the peptide at the LRP receptor. Later, cellular uptake assays confirmed higher cell uptake, demonstrating that Angiopep-2 binds to LRP receptors. The authors also assessed the permeability of MSN-based nanocarriers across the BBB using an *in vitro* BBB model. Results revealed that the smaller size and conjugation with Angiopep-2 promoted a greater permeability across the BBB. These findings demonstrate the potential of Angiopep-2-MSNs nanocarriers for drug delivery to the brain for further effective gliomas treatment.

Another interesting study on glioma treatment [81] investigated the inhibition ability of autophagy (protective mechanism for tumor cells) of 3-methyladenine (3-MA) using MSNs loaded with temozolomide (TMZ), coated with polydopamine (PDA), and modified with Asn-Gly-Arg (NGR). The modification of NGR ligand recognized the aminopeptidase N (cluster of differentiation 13) overexpressed in glioma cells, enhancing the accumulation of MSNs nanocarriers in C6 rat glioma cells. MSNs@TMZ@PDA@NGR multifunctional nanosystems exhibited a high apoptosis-inducing effect, compared with free TMZ, besides an antitumor effect enhanced by autophagy inhibition. This greater antitumor effect occurred because the autophagy inhibitors can block the antitumor drugs that cause autophagy in tumor cells,

enhancing the antitumor drug therapeutic effect. MSNs-based nanocarriers in combination with autophagy inhibitors characterize a new approach to glioma treatment.

Important advances have been demonstrated in Alzheimer's disease therapy using metal chelators associated with MSNs-based nanocarriers. Geng et al. [82] developed H_2O_2-responsive MSNs nanosystems functionalized with 3-carboxyphenylboronic acid and coated with immunoglobulin G (IgG) for targeted delivery of metal chelator clioquinol (CQ). Nanoparticles with a diameter of 100 nm and hexagonally arranged pores were obtained. In addition, the synthesis steps involving IgG and phenylboronic acid were successfully performed. The authors showed that the presence of H_2O_2 can trigger CQ release from MSNs due to boronate ester hydrolysis activated by H_2O_2. Moreover, MSNs containing CQ and IgG significantly inhibited the Aβ aggregation in the presence of H_2O_2, reducing neurotoxic ROS production, showing a similar behavior to that of CQ. The *in vitro* cytotoxicity using rat pheochromocytoma PC12 cells showed high cell viability, suggesting good biocompatibility of MSNs-CQ-IgG nanocarriers. These nanosystems represent a promising alternative application for Alzheimer's disease.

In another study, Yang et al. [83] engineered gold nanoparticle-capped MSNs nanocarriers as an H_2O_2-responsive release system for CQ delivery (labeled MSN-CQ-AuNPs). The authors exploited MSNs properties to enhance the chelator efficiency in the BBB as well as the potential of gold nanoparticles to inhibit amyloid-β peptide (Aβ) aggregation, an important Alzheimer's disease process. The MSN-CQ-AuNPs synthesis was successfully performed and characterized. The nanosystems showed a strong ability to cross the BBB by the *in vitro* co-culture model of the BBB, besides selective intracellular CQ release. Additionally, MSN-CQ-AuNPs inhibited Aβ aggregation, reducing cell membrane disruption and neurotoxic ROS formation, demonstrating its potential for Alzheimer's disease treatment.

3.8. Dermal route for MSNs administration

Skin drug release is a localized therapy, whose main aim is to minimize the side effects related to conventional drug administration routes. Different types of cells compose the skin, each having different functions and biochemical properties, in addition to containing a number of appendages, such as hair follicles, sweat glands, and nails [121]. In view of this, it is evident that the success of a treatment performed through this route depends on many factors, including the skin complex structure as well as the drug and carrier physicochemical properties.

Some challenges are mainly related to the skin barriers, which hamper drug permeation. Indeed, the skin is composed of three consecutive outer-to-inner layers: i) epidermis, ii) dermis, and iii) subcutaneous tissue, also called hypodermis (Fig. 5). The *Stratum corneum* (*sc*, or non-viable epidermis) is the outermost epidermis layer composed of low hydrated, flattened, and keratinized cells called corneocytes, which are embedded in a lipid matrix and organized in 15–25 layers of 10 μm in thickness, representing the most difficult barrier to drug permeation [122,123]. On the other hand, basal, spinous, granular, and lucid strata make up the viable epidermis.

It is worth highlighting that the drug transport mechanism through the *sc* occurs by passive diffusion taking place by three different routes as a function of the drug physicochemical properties, such as transcellular transport occurring through corneocytes, intercellular transport through the spaces between the corneocytes with partitioning into the lipid matrix, transfolicular transport through the hair follicles, and transglandular transport through the sudoriparous glands [125,126] (Fig. 6). However, in conditions of perfect skin integrity, transport occurs mainly through the appendages, intercellular and transcellular route, the latter being the least frequent transport [127].

Considering the difficulty of drugs permeating the skin, among several strategies proposed, the use of penetration enhancers and nanostructured systems seem to be the most effective. The properties of these systems, such as particle size, zeta potential, crystal structure, chemical composition, surface chemistry, and shape can influence their interactions with skin constituents. Regarding the percutaneous penetration of MSNs, some factors are pervasive considering the interactions with skin components. In addition to penetration enhancers, it seems that MSNs promote the drug diffusion across *sc* due to their nanometric size and high surface area. However, the drug penetration depth to viable epidermis and dermis is also dependent on vehicle solubility and the subsequent partitioning. Predominantly lipophilic vehicles penetrate the lipid-rich *sc* more easily, and the vehicle pH can ionize weak acid and basic drugs, hindering the drug permeation. The pH adjustment values also play an important role in MSNs stability because suitable surface charges are essential to keep them in dispersion, avoiding instability phenomena like aggregation, which impedes drug permeation mainly due to the increase in size [129].

According to Nigro et al. [130], the use of MSNs as a skin drug delivery system can be classified in terms of their applications as dermocosmetic [131], biomedical, and cancer treatments [132]. Other applications include transdermal drug delivery [133], gene delivery, and transcutaneous vaccination [134]. In the cosmetic field, MSNs can be considered a viable strategy to circumvent the toxicity issues related to inorganic compounds (ZnO and TiO_2) of sunscreens. In addition, MSNs can contribute to improving the stability of label natural active agents incorporating them into MSNs pores.

Ugazio et al. [86] reported the incorporation of an antioxidant quercetin (Q) into thermo-responsive MSNs to achieve effective skin release. Two types of MSNs were analyzed in terms of pore size, MSN_{small} (3.5 nm) and MSN_{big} (5 nm). Free radical copolymerization of N-isopropylacrylamide (NIPAM) and 3- (methacryloxypropyl)trimethoxysilane (MPS) inside the mesopores was conducted to modulate drug release in response to temperature stimulus. These polymers were chosen based on the premise that they suffer coil-to-globule transition in temperatures above the low critical solution temperature (LCST = 33 °C), in which the polymer chain shrinkage leads to about 90% of hydration loss, delivering therapeutic molecules. Overall, MSNs samples were 100–150 nm in size with regular and ordered channels with hexagonal symmetry. The Q loading from MSN_{small} was higher than that obtained with MSN_{big}. The authors attributed this behavior to the higher pore size unable to efficiently hold drug molecules. After functionalization, a decrease in Q loading was observed for both samples in response to the grafted copolymer hindrance. The slower Q release from functionalized MSNs, in comparison with bare MSNs, suggests a stronger drug-matrix interaction. Further, an *in vitro* Q release assay was evaluated in temperatures below (20 °C) and above (40 °C) LCST, showing that polymer chains really respond to temperature stimuli, releasing the flavonoid molecules immobilized within the mesopores. It was interesting to observe that no Q permeation performed at Franz vertical cells with porcine skin was verified in the receptor medium after 24 h, which was attributed to *sc* resistance as well as the physicochemical characteristics of this flavonoid. In relation to Q retention by porcine skin, Q/MSN_{big} showed higher retention than Q/copoly-MSN_{big}, in agreement with the faster Q release rates, increasing the Q availability to the *sc*. Both samples displayed biocompatibility with immortalized human keratinocytes (HaCaT).

Another noble function of MSNs administration through the cutaneous route is that it circumvents the drawbacks related to the side effects exacerbated by the systemic exposure. Sapino et al. [87] explored this strategy to deliver methotrexate (MTX), a folic acid antagonist showing cytotoxic activity, to treat skin disorders. The particles prepared had an average diameter of 200 nm with a zeta potential of −21.6 mV related to the silanol groups; however, this value decreased to −16.1 mV after MTX incorporation, meaning that silica hydroxyl groups are involved in noncovalent bonding with MTX. The amount of MTX loaded in MSNs was about 39.4%. The *in vitro* release profile under physiological conditions showed that MTX/MSN was able to prolong the MTX release rates, compared to free MTX, due to the weak drug-matrix interactions. An *ex vivo* porcine skin study using Franz cells was

performed to test free MTX and MTX/MSN incorporated in different dermal formulations, namely phosphate buffer, pure shea butter, glycerolipidic lotions, and some oil-in-water (O/W) and water-in-oil (W/O) emulsions. High MTX permeation values (from 6.52 to 6.56 μg cm^{-2}) were reached from glycerolipidic lotions, recognized for favoring permeation. Higher MTX epidermal retention was observed in skin slices from the nanosized complex than that of free-MTX, which was related to the greater intercellular penetration and increased surface area of the nanosized carriers. Later, porcine dermatomed skin was examined by scanning electron microscopy (SEM) after 24 h of MSNs application, demonstrating the presence of silica aggregates with a micrometric range in the epidermis. The authors concluded that such silica aggregate can slow systemic absorption and act as a prolonged-release deposit of the incorporated drug.

Cancer therapy is still a great challenge. Photodynamic therapy (PDT) has gained attention due to its non-invasive character and generation of highly toxic, effective ROS in solid tumors. 5-Aminolevulinic acid (5-ALA) shows many advantages over other photosensitizers due to its nontoxicity and quick excretion from biological systems. However, 5-ALA shows hydrophilic property and low specificity to cancer cell, impacting on bioavailability. Therefore, Ma et al. [88] developed hollow MSNs (HMSNs) to overcome the lipophilic barrier and facilitate the entry of 5-ALA into skin cancer cells. The functionalization with folic acid (FA) as a cancer-targeting ligand was explored to facilitate the internalization of HMSNs. Particles exhibited 150 nm in size with a mesoporous shell thickness of 30 nm, besides pore sizes ranging from 2.1 to 2.7 nm. In order to investigate the target delivery of HMSNs, cells with low (normal HEK293 cells) and high (B16F10 skin cancer cells) FA receptor (FAR) expression were used. Functionalized samples (HMSN-FA) were labeled with fluorescein isothiocyanate (FITC). When the results of the two cell lines were compared, a remarkably higher uptake of HMSN-FA-FITC was observed in B16F10 cells than in HEK293 cells, confirming the targeted delivery capability attributed to the FAR meditated endocytosis. Further, the *in vitro* protoporphyrin IX (PphIX) generation was investigated by confocal laser scanning microscopy (CLSM). Interestingly, any red fluorescence color could be seen in HEK293 normal cells, in contrast to B16F10 skin cancer cells, where red fluorescence was more intense from 5-ALA@HMSNP-PEG + FA than from free 5-ALA. Photocytotoxicity was investigated by a 3-(4,5-dimethylthiazol-2-yl)-5-(3-carboxymethoxyphenyl)-2-(4-sulfophenyl)-2 H-tetrazolium (MTS) assay, and results for non-irradiated samples showed that ALA@HMSNP-PEG + FA was biocompatible. However, light irradiation led to cell viability decrease, which occurred in a dose-dependent way.

It is known that small interfering RNA (siRNA) is a promising tool for skin squamous cell carcinoma (SCC) treatment because of its interference with specific gene expression related to this disease. However, properties such as siRNA size (10–20 kDa) hinder the skin permeation. Lio et al. [89] developed a topical formulation based on MSNs for siRNA transdermal delivery aiming to facilitate skin cancer treatment. MSNP-MB (MB = molecular beacon, a model of oligonucleotide) was built and further coated with poly-L-lysine (PLL) converting particles to cationic ones, showing a pore size of 4 nm, particle sizes of 200 and 250 nm, and zeta potential of −19 and −34 mV, before and after complexation. However, PLL coating caused the zeta potential to rise to + 30 mV. In *in vitro* release tests, 65% of MB was released within 6 h of testing, and PLL coating showed no interference in the release profile. It seems that the MSNPs-MB-PLL positive charges were responsible for the greatest nanosystem internalization and MB concentration in the cells, confirmed by its recognition of cellular GAPDH (Glyceraldehyde 3-phosphate dehydrogenase, a kind of mRNA) mRNA following MSNPs-MB-PLL delivery. Higher fluorescence levels were observed in mice via IT injection, followed by those under topical application in a SCC xenograft model. However, MSNSPs-MB-PLL was responsible for the lowest stain Cy5 distribution in all major organs. In the topical delivery of siRNA with MSNPs for skin tumor treatment, the siRNA release rates were the same as those of MBs, and TGFβR-1 gene expression in RT3 cells was reduced by 60% relative to the control.

The use of MSNs has also been explored for the topical administration of anesthetics on the skin. In a study developed by Nafisi et al. [90], lidocaine (LIDO)–a member of the Caine Family used as topical anesthetic showing both poor aqueous solubility and negligible skin uptake–was incorporated into MSNs (3/1, 2/1 and 1/1 ratios) and functionalized with positively charged amino-propyl groups (NH_2) as a strategy to enhance the LIDO permeation into the skin. MSNs showed sizes ranging from 45 to 95 nm and distinct zeta potential as a function of NH_2 functionalization (non-functionalized samples from −35 to −19 mV due to Si–OH groups), with values ranging from +23 to +33 mV in amino-functionalized samples. Pores sizes were 0.23–2.61 nm. An *in vitro* LIDO delivery study was performed using a cellulose dialysis bag immersed in phosphate buffer saline with the 1/1 functionalized samples (encapsulation efficiency [EE] of 99.73%) and non-functionalized MSNs (EE of 94.40%). Dissolution LIDO rates from MSNs and NH_2-MSNs were faster than pure LIDO, the achieved percentage being 38, 60, and 28% after 7 h, respectively, in accordance with the therapy requiring a quick onset of anesthetic effect. *Ex vivo* skin permeation was carried out in vertical diffusion Franz cells by means of skin from an abdomen reduction surgery. Like the *in vitro* drug release, amino-functionalized MSNs also enhanced LIDO permeation, so 64% of the drug content was released in 24 h, while LIDO release was 13% from the bare MSNs. The authors attributed this behavior to the electrostatic interactions occurring between the sample positive charges and the skin negative charges, confirming the importance of NH_2 functionalization. Other studies exploring the use of MSNs can be analyzed using Table 1.

3.9. Oral route for MSN administration

Among all drug administration routes, the oral way remains the most accepted route mainly by patients in chronic disease treatment, since it has important advantages that make administration easier, with its non-invasive and safer route [135,136]. It allows greater dosage flexibility, therapeutic classes, and different dosage forms. In addition, there is no need for administration to be performed by a specialized professional or in a hospital environment, contributing to a reduction in the overall treatment costs. Besides, in economic terms, the pharmaceutical dosage forms for oral administration do not require aseptic and/or sterile conditions for their production [137].

Despite the important advantages of this administration route, drugs administered orally must overcome different barriers imposed by the GIT in order to exert their therapeutic effect, be it local or systemic. In terms of the systemic effect, it is known that the drug must be absorbed into the bloodstream, occurring most often through the small intestine, which has a high absorptive capacity and extensive surface area (300–400 m^2) due to villi and microvilli present on the surface of intestinal cells (enterocytes). Only after this previous stage can the drug be distributed to the different tissues, reaching the target site. However, due to the long path traveled by the drug and considering possible losses, whether due to problems of molecule instability and/or permeability or by interacting with different compounds present in the GIT, high doses of these drugs must be administered to achieve therapeutic concentrations, which are associated with increased toxic effects. The same should be considered when it comes to the local effect, since depending on the drug origin, it may undergo enzymatic digestion (anti-hyperlipidemic agents, cephalosporin antibiotics, proteins, and peptides) or chemical degradation in the upper GIT portions with acid pH [136], like artemether, erythromycin, and candesartan cilexetil drugs [135].

Indeed, it can be inferred that the therapeutic effect of the drug administered orally depends on the physiological barriers imposed by the GIT, the drug physicochemical properties (solubility [log-P], particle size, and acid dissociation constant [*pKa*]) and the biopharmaceutical properties (permeability, metabolization, and efflux mechanisms), remaining a scientific challenge.

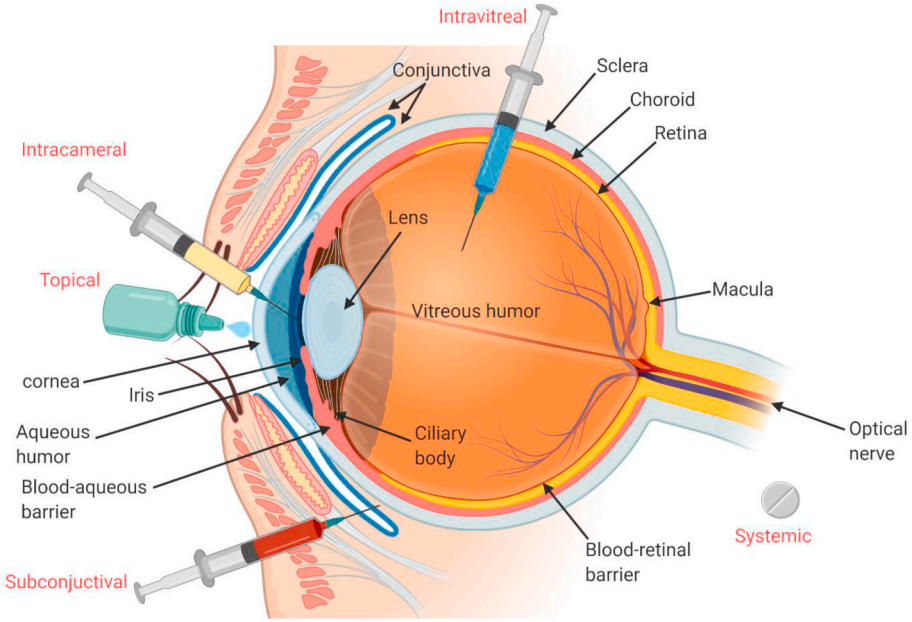

Fig. 2. Schematic representation of eye anatomy and physiology indicating the barriers to ocular absorption and the possible ophthalmic administration routes.

GIT can be divided into three main portions, namely stomach, small intestine (consisting of duodenum, jejunum, and ileum), and large intestine (or colon) (Fig. 7). For each of these sections, different motility patterns, transit time, pH values, fluid volume, and viscosity, diversity of microbiota, and enzyme content are found, in which drugs must be resistant without activity loss [138]. In addition, it is worth mentioning that there is great inter-individual variability related to these factors, which are intensified mainly when individuals of different race, sex, and age groups are compared, and to some pre-existing diseases. The food presence in the GIT must also be considered, since drugs can interact with certain compounds, changing their bioavailability [139,140].

Therefore, in a sequence of successive events occurring after oral administration, the drug must resist the acid attacks in the stomach (pH values ranging between 1.5 and 5 for the fasted and fed state, respectively), as well as digestion by enzymes present in the stomach (pepsin) and small intestine (trypsin, chymotrypsin, amylase, lactase, carboxypeptidase, and lipase) [141]. The drug must also pass through the mucus layer (diffusion across mucus) that coats the GI epithelium, establishing direct contact with the intestinal membrane being absorbed from the lumen for systemic circulation through different mechanisms of cell transport [142].

However, even if all the steps mentioned above are successfully completed, drug transport across the intestinal membrane may still be limited by efflux mechanisms through transporters present in the cell membrane, such as glycoprotein P (P-gp) [143], as occurs with the digoxin, PTX, and DOX drugs [144]. Even though absorption occurs, hepatic metabolism may be responsible for the reduced bioavailability of several drugs [145]. The first pass (hepatic) metabolism of anti-hypertensive, cardiovascular (b-blockers, calcium channel blockers, ACE inhibitors), and anti-diabetic agents (repaglinide) are responsible for their low oral bioavailability [135].

Regarding physicochemical drug properties (solubility, molecular weight, and stability), it is known that most drugs are weak acids or basics that undergo ionization at different pH values found throughout the GIT, affecting their stability, solubility, and the consequent bioavailability. In fact, to achieve therapeutic effect after oral administration, a drug must be in solution in the gastrointestinal fluids for the absorption to occur [137]. Sodium diclofenac (SD) is a classic example, as this weak acid with *pka* of 4.15. SD can suffer great dissociation at pH values above *pKa* (in the small intestine), which explains why this drug is released in greater amounts in this GIT portion.

Special classes of bioactive molecules, such as biotherapeutics based on peptides and proteins, deserve greater attention when administered orally. These macromolecules are generally not stable in stomach acid pH, undergoing conformational changes and being digested by the proteolytic enzymes present in the stomach and small intestine. The activity loss is accompanied by a low intestinal permeation capacity as these are molecules of high molecular weight and high hydrophilicity, requiring their incorporation into sophisticated release systems providing both protection and release kinetics control [146,147], such as those associated with absorption enhancers, enzyme inhibitors, mucoadhesive systems, and systems with enteric coating.

Despite the oral route being the most widely accepted, promoting greater adherence to treatment by the patient, oral absorption is a challenge. Nanometric-size drug delivery systems, which can be polymeric, inorganic, and lipid-based, can play a key role in favoring a bioavailability increase and stability following oral administration [135]. However, according to Florek et al. [137], only a few of them meet commercialization requirements.

MSNs have been proven to be a promising oral drug delivery system due to their tunable properties, like controllable pore size, high drug loading, porosity, and controlled release kinetics [148], besides being biocompatible. It is known that among all the factors that contribute to reduced oral bioavailability, the low solubility of some drugs is among the most important. However, drug-loaded MSNs can overcome these problems, since drugs become confined in a nanosized environment with increased solubility due to the high surface area, and drug-carrier interactions change the drug physical state from crystalline to amorphous, thus contributing to enhancing drug delivery rates [149].

Another remarkable advantage of MSNs for oral delivery is their easy functionalization due to the presence of silanol groups on the surface, which have been related to an increase in drug loading capacity, as well as greater release kinetics control. This is due to the establishment of stronger drug-carrier interactions, such as electrostatic interactions, achieved through functionalization with ionic groups [137]. Many factors also influence the drug loading into MSNs, such as adsorption time, temperature, loading solution pH, and concentration [150].

In order to overcome the poor aqueous solubility of Indomethacin (IMC), Zhang et al. [96] fabricated mesoporous silica nanorods (MSNRs) as a strategy to improve oral bioavailability and evaluate the shape

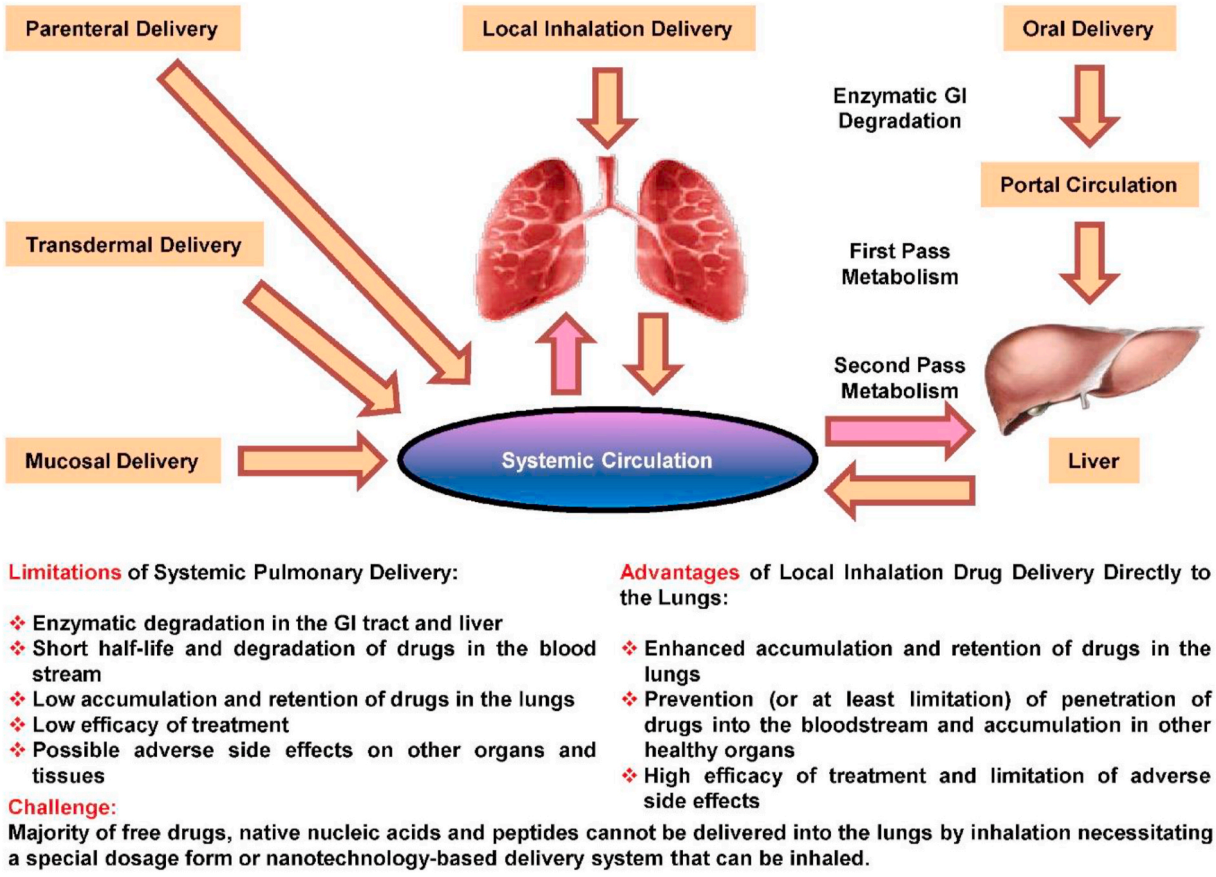

Fig. 3. Advantages (local delivery), limitations (systemic delivery), and challenges of pulmonary drug delivery [116].

effects of MSNs on oral delivery. Results showed low values of drug loading (~29 and 22% for MSNRs and MSNs, respectively), but an excellent dissolution-enhancing effect (100% of IMC release after 1 h). *In vitro* IMC release was governed by diffusion due to the mesostructure, related to both the IMC incorporation into MSNRs in an amorphous state and the hydrophilicity of the silica surface. Regarding the faster IMC release from MSNRs than from MSNs, the larger pores of the former, along with the more ordered helical channels, are known to facilitate the drug release. This set of results led to better oral IMC bioavailability.

Although several organic nanoparticles are currently used as an alternative to enhance the oral bioavailability of CUR, these systems present many instability issues, making the proposal unfeasible. Hartono et al. [97] explored the conjugation of CUR with amino-functionalized MSNs with 3D interconnected large pore size (10 nm), originating new composites with different particle sizes, namely micron-sized-particles (MSMs with 1 μm) and MSNs (100 nm). The amino-functionalized MSNs successfully controlled the CUR release rates, with the release profile reaching a plateau after 48 h. MSNs were responsible for the higher CUR release amount relative to MSMs, which is in accordance with their lower particle size and, consequently, higher surface area. Likewise, the solubility test followed the same trend, so MSNs-CUR showed solubility twice as high as that exhibited by MSMs-CUR. These results contributed to the bioavailability enhancement in mice after oral administration with equal t_{max} (time to reach the maximum concentration) of 3 h, but MSNs showed higher CUR concentration in plasma (C_{max} = 0.0291 μg mL^{-1}), compared to MSMs (C_{max} = 0.0105 μg mL^{-1}).

Later, some authors also investigated the therapeutic effects (anti-inflammatory activity) of CUR orally administered through MSNs [151]. MSNs were prepared as a cubic mesostructure of 100 nm in size and pore size of 10 nm, besides 3-aminopropyl-triethoxysilane (APTES) functionalization (amine groups). An *In vivo* study was performed by induction of carrageenan in Wistar rat feed, and results showed that CUR-MSN was responsible for the lower percentage of edema formation than that of free CUR and SD (positive control). This behavior may be attributed to the enhancement of CUR aqueous solubility and bioavailability. Interestingly, MSNs-CUR showed almost the same ulcerogenic index (2.32 ± 0.82) as the negative control group (2.00 ± 0.00), suggesting its importance in side effects reduction. To confirm this hypothesis, the authors compared the MSNs-CUR result with the ulcer index found for SD, which was almost three times higher (6.16 ± 0.41). Another study on CUR can be found in Gao et al. [98].

The effects of MSNs on the oral bioavailability and intestinal Telmisartan (TEL) permeability were investigated by Zhang et al. [99] and compared with commercial Micardis®. TEL release was significantly improved from MSN, compared to Micardis®, in phosphate buffer (pH 6.8). The authors attributed this behavior to the pore channels that change the crystalline drug state to an amorphous phase of enhanced dissolution. Likewise, it seems that the shorter pore channel length of MSNs facilitates drug molecule diffusion due to the shorter pathway to the dissolution medium. It is worth noting that MSNs internalization with different particle sizes (20, 60, and 90 nm) into Caco-2 cells after 1 h of incubation by CLSM displayed higher accumulation in the cell membrane region without reaching the nucleus. In addition, transmission electronic microscopy (TEM) was able to demonstrate the endocytoses of MSNs by Caco-2 cells after binding to intestinal villi. The MSNs uptake was time-, concentration-, and size-dependent. Regarding the intestinal permeability, TEL transport was linear, increased by the P-glycoprotein inhibitor (cyclosporin A) and MSNs use, suggesting that both decreased the P-gp-mediated drug efflux.

Recently, the antigen stability and immune response intensity against the recombinant subunit of cholera toxin (CTB) were also

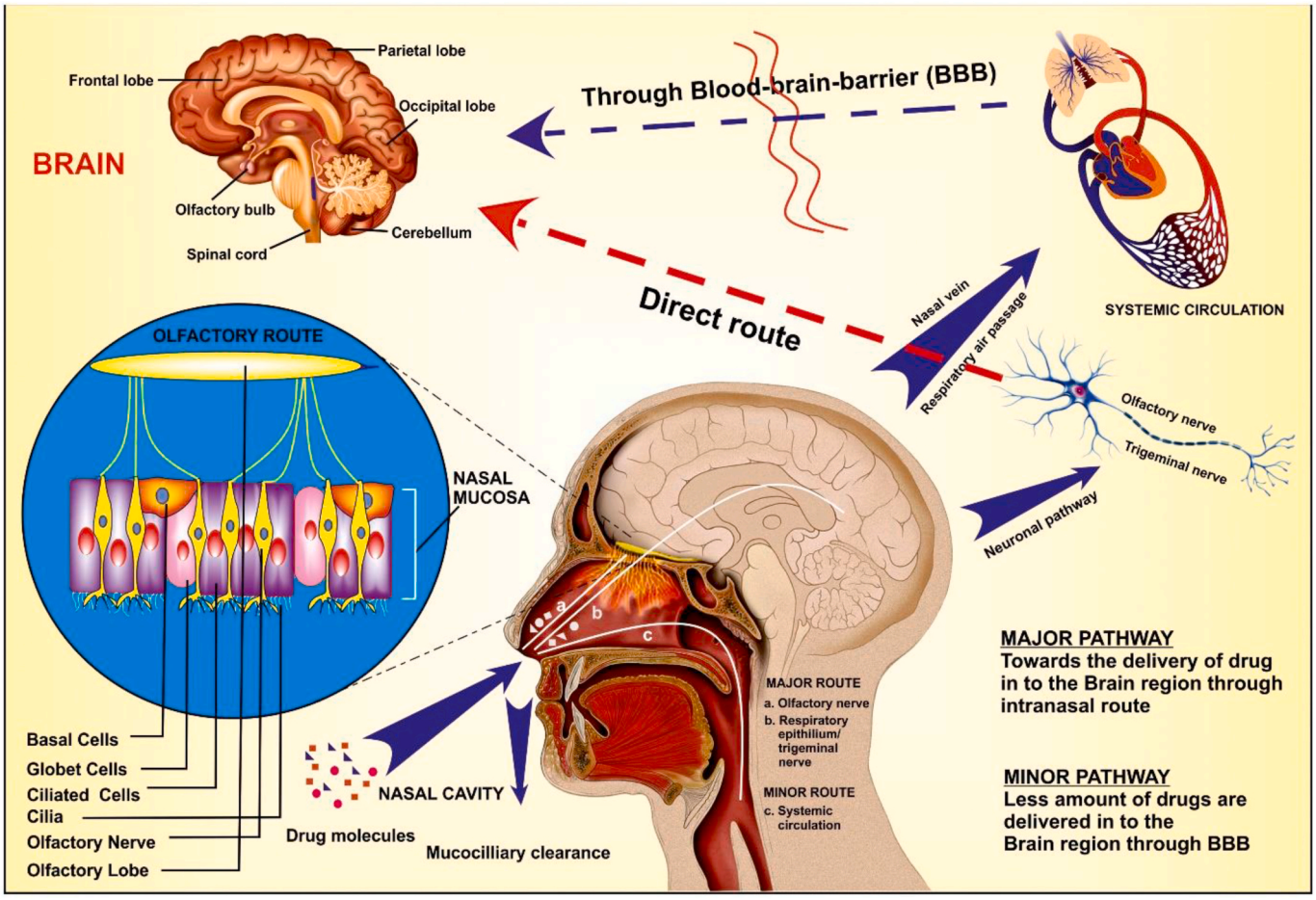

Fig. 4. Nasal cavity structure (respiratory epithelium and olfactory nerves) demonstrating the drug transport pathways from nose-to-brain: the intranasal route through the olfactory and respiratory region (major pathway) and the systemic circulation by crossing the BBB (minor pathway). Reproduced with permission [118]. Copyright 2018, Elsevier.

investigated by exploring the MSNs unique properties [100], considering the need for special carriers intended to improve gastrointestinal protection and vaccine potency. Indeed, the oral vaccine can be optimized by exploring the endocytosis particle uptake occurring in M cells associated with immune response. According to the results, MSNs are advantageous over polymeric and lipid-based nanoparticles, which hydrolyze in the harsh GIT conditions. Characterization results showed that MSNs were spherical, exhibiting 350–500 nm in size with an average pore diameter of 8 nm. MSNs were able to control CTB antigen release rates for 12 days, with only 25% of the loaded antigen being released in the first 24 h. After rabbit immunization by the oral route, IgG titration response exhibited an elevated antibody response for MSN-CTB after the 4th week, while free-CTB was devoid of any response. In addition, anti-CTB IgA response of immunized rabbits evaluated from saliva and vaginal secretions displayed an intense IgA response superior to the already marketed Dukoral® vaccine. This impressive behavior was ascribed to the suitable CTB antigen protection and the target-specific delivery to the M cells.

Despite MSNs unique properties, few works have described their biodistribution and toxicity after oral administration. Li et al. [101] proposed an interesting study about the impact of three types of MSNs shapes on *in vivo* behavior, which varied as a function of aspect ratios (AR). MSNs with AR equal to 1 were considered spherical (labeled NSs), those with AR equal to 1.75 were considered short-rod (labeled NSRs), and those with AR equal to 5 were considered long-rod (labeled NLRs). Media simulating the stomach, intestine, and body fluids were used as a reference for the study of *in vitro* biodegradation, followed by the incubation of 2 mg mL^{-1} of samples in them (37 °C and 150 rpm min^{-1}). After 7 days, low biodegradation in acid medium (lower than 10%) was detected for all MSNs, while an increase of 62, 29, and 17% for NSs, NSRs, and NLRs was observed for intestinal medium, respectively. This behavior makes this nanosystem applicable as an oral delivery system that protects drugs in the stomach area, promoting intestinal release, which is very important for biotechnological actives. However, *in vivo* studies showed that all three-shaped MSNs are absorbed into systemic circulation with an observable distribution in the liver, lung, spleen, and kidney.

It is important to bear in mind that these MSNs global performance can be totally changed by the simple functionalization with specific molecules, contributing to effective targeting or solubility and permeability enhancement. Different molecules can be explored for silica functionalization, such as polymers resistant to the harsh stomachic environment (cellulose acetate phthalate and hydroxypropilmethylcellulose phtalate) and polymers with pH-dependent solubility, to explore the pH gradient along the GIT as a release-trigger mechanism (alginates, pectin, and gellan gum). Bioadhesive molecules, such as cationic polymers like chitosan, which electrostatically interacts with mucin (negatively charged), has also been used, increasing the system permanence time at the target site and, consequently, the bioavailability.

Following this concept, Guha et al. [102] developed pH-dependent cylindrical MSNs to deliver insulin (INS) orally by coating the particles with poly-(methacrylic acid-co vinyl triethoxylsilane) without presenting cytotoxicity. The final coated sample had a pore diameter of

about 65 nm and entrapment efficiency of 39%. Interestingly, the coating was responsible for the pH-dependent INS release, being more pronounced at intestinal (pH 7.4) than stomachic pH (only 13% of insulin released after 2 h in pH 1.2), which should contribute to its protection against acid denaturation and enzymatic degradation in upper GIT portions. The hypoglycemic profile tested in rats with streptozotocin-induced diabetes showed a fall of about 60% in blood glucose levels after 6 h of coated-MSNs oral administration owing to INS protection against degradation.

Another type of lipidic coating was performed by sonicating a mixture of liposomes and MSNs for oral delivery of ciprofloxacin (CIP) for the intracellular elimination of *Salmonella* [103]. Particles (lipid coated MSNs [L-MSNs]) had 50–100 nm in diameter with a lipid coat thickness of 5 nm. Interestingly, liposome fusion on MSNs surface was able to prolong the CIP release rates, so after 30 min only 30% of the drug was released, against 90% for uncoated MSNs, meaning that lipid countered the molecule diffusion to the elution medium. As a consequence, antibacterial activity was higher compared with free CIP. *Salmonella* intracellular proliferation inside the host cell was evidenced in untreated samples with lower fold change from L-MSNs@CIP in both RAW 264.7 macrophage cells and HeLa cells. L-MSN uptake observed by confocal analysis increased after 4 h of treatment, the antibacterial activity enhancement being attributed to the intracellular accumulation of L-MSNs in *Salmonella typhimurium*. These findings converged to excellent *in vivo* antibacterial results, measured in terms of mice survival after *Salmonella* infection. Lower doses of L-MSNs@CIP were as effective as free CIP administered at twice the concentration [103].

An interesting study explored the chirality of structures as a mechanism to differentiate nimesulide (NMS) release profile from MSNs [104]. The authors synthesized functional MSNs (F-MSNs) with molecular level chiral function property, namely levorotatory MSNs (FL-MSNs) and dextrorotatory MSNs (FD-MSNs). Spherical MSNs with a rough surface of about 200–300 nm in size were prepared; however, no morphological differences were observed between them. Both samples incorporated the same drug amount and no crystalline peak was observed in X-ray diffraction (XRD) analysis, demonstrating the amorphous nature of the incorporated drug. Differences were not observed between the drug release profiles from FL-MSNs and FD-MSNs. However, the chiral *in vitro* medium was also evaluated using two kinds of chiral dissolution medium, one at pH 6.8 PBS containing 0.5 mg mL^{-1} L-Alanine (L-Ala-PBS) and the other at pH 6.8 PBS containing 0.5 mg mL^{-1} D-Alanine (D-Ala-PBS). As expected, a higher drug release was observed from FL-MSNs in L-Ala-PBS and FD-MSNs in D-Ala-PBS, i.e., each carrier responded to the corresponding chiral medium. In addition, FD-MSNs were considered the best carriers, since higher drug amounts were released. According to the paw edema degree of rats, both NMS-loaded FL-MSNs and NMS-loaded FD-MSNs had stronger anti-inflammatory action; however, the swelling inhibition rate of FD-MSNs was 1.5 times stronger than that of FL-MSNs.

4. Biological behavior of MSNs

The successful application of MSNs as versatile drug carriers requires a deep understanding of the interactions between MSNs and biological systems. Physicochemical properties such as size, shape, and surface chemistry can dramatically influence the MSNs behaviors in biological systems and might, in part, determine their biocompatibility, biodistribution, biodegradability, and clearance [28,152].

4.1. Biocompatibility and biodistribution

The biocompatibility and biodistribution of any carrier are a prerequisite property of any pharmaceutical product to ascertain that these products do not accumulate in the body over a period of time causing untoward effects. Fu et al. [112] studied the toxicity of MSNs with a particle size of 110 nm in ICR mice. Following administration via hypodermic, IM and IV injections as well as oral administration, the *in vivo* distribution of fluorescent-tagged MSNs was tracked. MSNs administered via IV route were found to preferentially accumulate in the liver and spleen at the end of 24 h and 7 days whereas those administered by other routes did not show any fluorescence in these organs. A portion of the MSNs administered via the IM and hypodermic routes could cross different biological barriers with a slow absorption rate. No histopathological changes were observed in the liver, spleen, kidney, or lung at the end of 24 h and 7 days by different exposure routes. These results suggested that MSNs were safe and well-tolerated when administered by oral and IV routes.

Surface properties have a great impact on the MSNs biocompatibility and biodistribution. The main toxicity pathway associated with these nanosystems is due to their surface chemistry (silanol groups), which can interact with the membrane components leading to cell lysis and leaking of the cellular components [152,153]. Functionalization with polyethylene glycol (PEG) helps the MSNs to escape, being captured by the liver, spleen, and lung tissues [154]. Yu et al. [155] studied the surface features of silica nanocarriers on cellular toxicity. After 72 h exposure, cancer epithelial (A549) cells were resistant to the nanoparticles even at a concentration of 500 μg mL^{-1}. However, at 1000 μg mL^{-1}, observable toxicity was seen. It was observed that amino-modified MSNs showed a higher level of cellular association. This higher interaction between amino MSNs and cells could be associated with a particular surface threshold beyond which cell interaction is facilitated.

Nanoparticle size also has a profound influence on the MSNs biodistribution. MSNs with particle size from 80 to 360 nm were administered to ICR mice. An increase in particle size led to an increase in its accumulation in the liver and spleen following IV administration. However, no pathological abnormalities were observed at the end of 1 month [154]. Zhang et al. [156] synthesized DOX-loaded MSNs functionalized with folic acid sizes varying from 48, 72, to 100 nm and investigated the particle size effect on its *in vivo* distribution in MDA-MB-231 tumor-bearing Balb mice. It was observed that MSNs with a size of 48 nm showed the highest accumulation in the tumor tissues.

4.2. Biodegradability

The silica particles do degrade into silicic acid ($Si(OH)_4$, *pKa* of 9.6) in biological media by dissolution. Silicic acid is soluble in water and consists of the dominant silicon species at low concentration ($<2 \times 10^{-3}$ M) [14]. It is also excreted through the urine and its good bioavailability even contributes to maintaining bone health [14,25]. Investigations have been carried out to assess the direct influence of the size, morphology, and degradation medium parameters on the silica nanoparticle degradation. The physicochemical engineering of MSNs thus allows one to tune the dissolution silica rate in biorelevant media for specific biomedical applications [14].

4.2.1. Effect of size

Chen et al. [157] showed that MSNs degradation is independent of their diameter with 390, 310, 200, and 150 nm nanoparticles in simulated body fluid (SBF) at 37 °C. During the first two days, the degradation rate was nearly 45% per day, which then slowed down to about 1% per day, and the degradation was completed in a week.

4.2.2. Effect of surface area

He et al. [158] investigated the role of the surface area on the mesoporous silica degradation, comparing three samples of 958, 829, and 282 $m^2\ g^{-1}$ at a fixed concentration of 0.1 mg mL^{-1} in SBF, sealed in polyethylene bottles at 37 °C and shaken at 150 rpm with a mechanical shaker. This study indicated that, on the one hand, there was a burst degradation in the first 2–4 h, leading to 30, 70, and 90% of silica hydrolytic degradation as the surface increased, and, on the other hand, a complete degradation was obtained in 15 days.

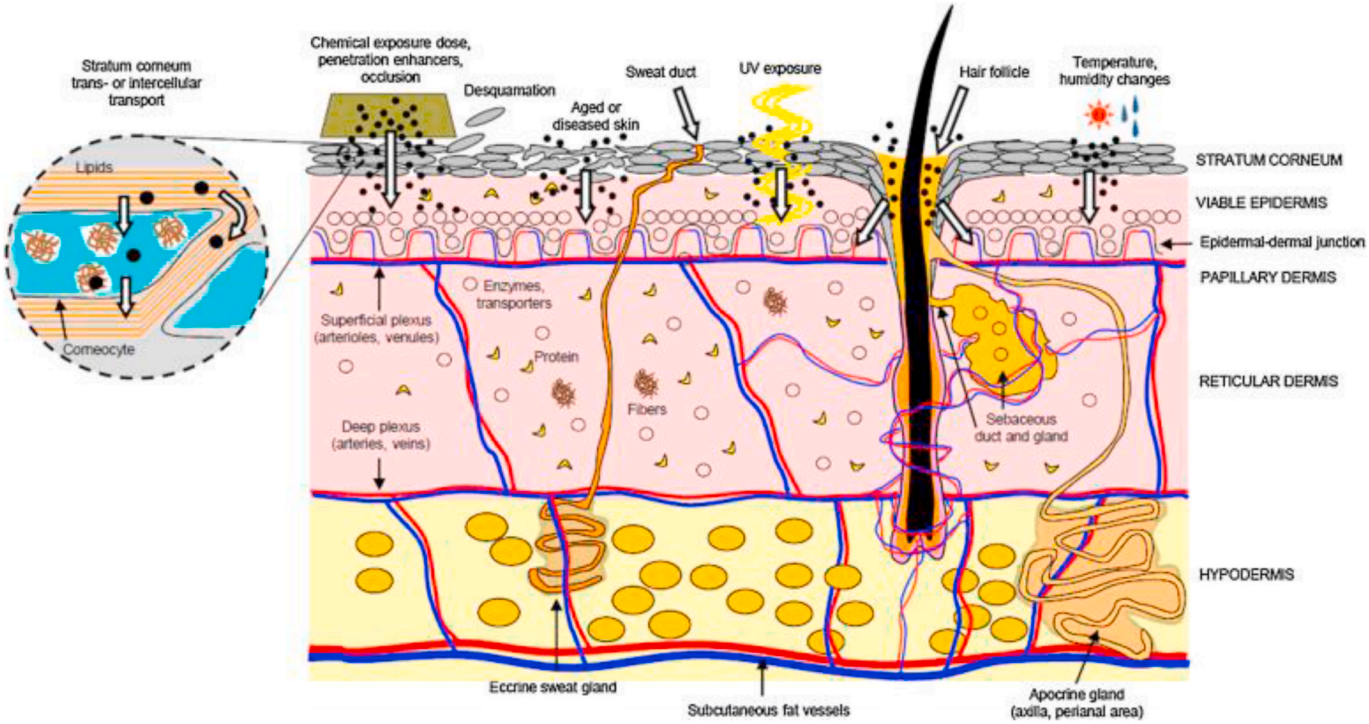

Fig. 5. Schematic overview of the skin layers and interfering factors/mechanisms of drug transport across the skin. Reproduced with permission [124]. Copyright 2015, Elsevier.

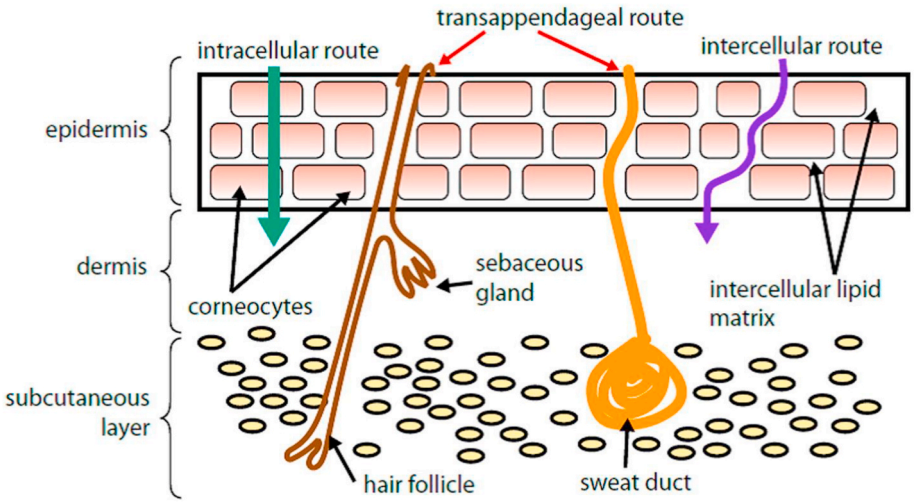

Fig. 6. Routes of percutaneous absorption. Reproduced with permission [128]. Copyright 2016, Elsevier.

4.2.3. *Effects of morphology and degradation medium*

Li et al. [101] reported the MSNs degradation with spherical and rod-shaped morphologies with aspect ratios (ARs) of 1.75 and 5. They investigated these nanoparticles by TEM and sample weight measurements after degradation for 7 days by soaking in three different degradation media: simulated gastric fluid (SGF, pH 1.2), simulated intestinal fluid (SIF, pH 6.5), and SBF (pH 7). The degradation was much more pronounced and AR-dependent in simulated intestinal and body fluids. In general, the SIF generated more degradation than the SBF. The authors also showed that spherical MSNs were more rapidly degraded than rod-like MSNs with ARs of 2 and 4, and the presence of FBS in Dulbecco's modified Eagle medium (DMEM) accelerated the degradation process [25,159].

4.3. *Clearance*

The MSNs ingested by humans circulate through the blood plasma and are absorbed in the form of silicic acid. After that, MSNs are excreted mainly by the renal clearance route, urine (~73%), but also feces (~21%). The particle dissolution into silicic acid and its subsequent excretion was demonstrated *in vivo* on mice models and in human clinical trials [25,85,160]. Several trends have been observed between the MSNs characteristics and their clearance: i) the effect of size, ii) the effect of surface functions, iii) the effect of surface charge, and iv) the effect of morphology.

4.3.1. *Effect of size*

Silica-based nanoparticles with sizes ranging from 100 to 400 nm

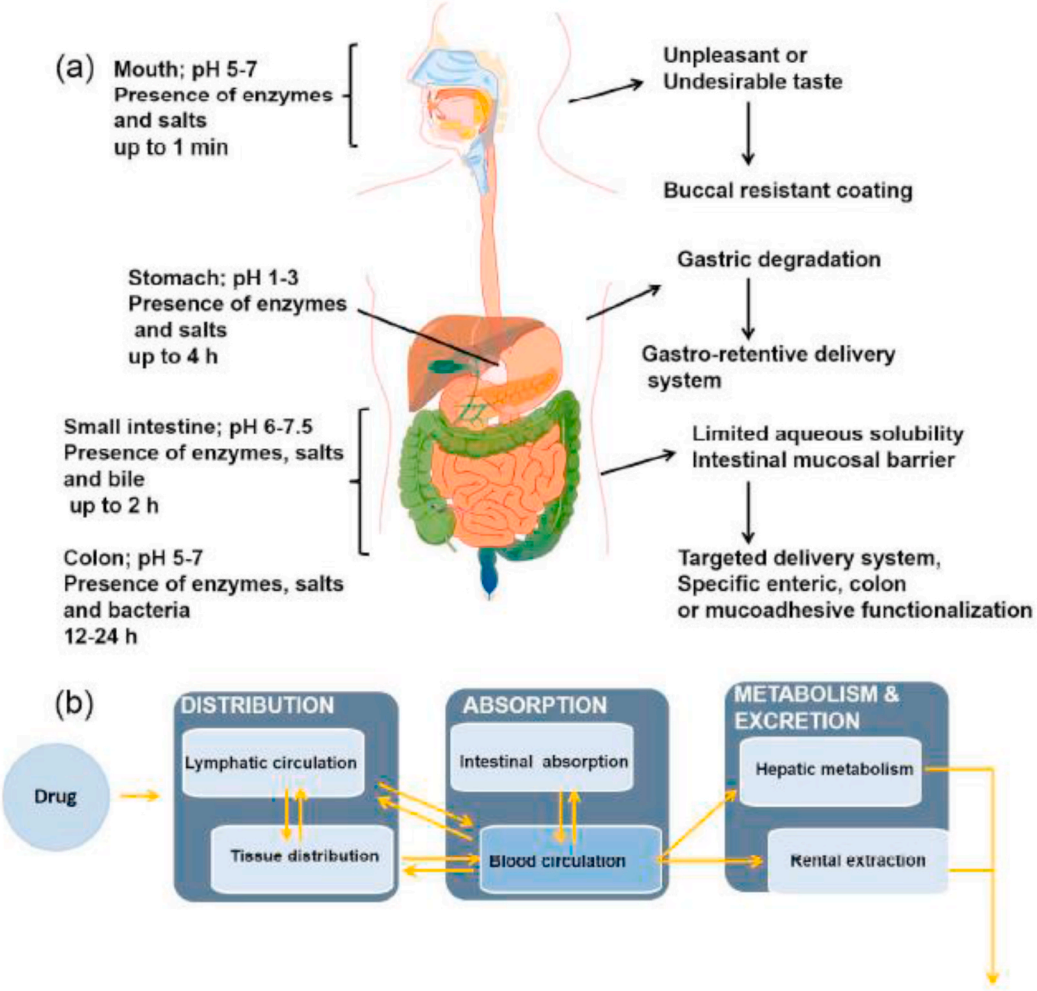

Fig. 7. Different sections of GIT and their main properties. Reproduced with permission [137]. Copyright 2017, Royal Society of Chemistry.

were increasingly captured by the reticuloendothelial system organs as the size increased [25,26].

He et al. [154] reported a study where MSNs of various sizes (80, 120, 200, and 360 nm) presented a significant nanosystem excretion of 15–45% after the first 30 min. Kumar et al. [161] showed that MSNs with sizes of 20–25 nm preferred hepatobiliary excretion, with a complete clearance over a period of 15 days [25,154]. Cho et al. [162] studied nonporous silica nanoparticles of 50, 100, and 200 nm and demonstrated that their clearance occurred in the urine and the bile. The nanoparticles with a smaller size were excreted faster [14,25].

4.3.2. *Effect of surface functions*

It was demonstrated that PEGylated nonporous silica nanoparticles had longer blood circulation times ($t½ = 180 \pm 40$ min) than unmodified silica ($t½ = 80 \pm 30$ min) and carboxylated silica particles ($t½ = 35 \pm 10$ min), and were partly excreted via renal clearance [14,25,163]. A stealth behavior is acquired by PEGylation, which reduces the RES uptake and increases the circulation half-life. As a result, PEGylated MSNs of various sizes (80, 120, 200, and 360 nm) were excreted more slowly than unfunctionalized ones due to the much slower particle capture by the liver and spleen. This trend was also observed in the MSNs [154].

4.3.3. *Effect of charge*

The surface charge has a key impact on the adsorption of lipoproteins circulating in the bloodstream and plays a critical role in the nanoparticles (NPs) excretion from the body [14,25,161]. Souris et al. [164] studied for the first time the charge influence on the MSNs excretion. MSNs with a highly positive charge (zeta potential of +34 mv at pH 7.4) were rapidly excreted from the liver into the GIT and then eliminated via feces, while negatively charged nanoparticles (zeta potential of −18 mv at pH 7.4) remained sequestered within the liver.

4.3.4. *Effect of morphology*

The morphology influence on the clearance showed that MSNRs of aspect ratio ~1.5 (185 nm ± 22 nm long) are more rapidly cleared than longer nanorods of aspect ratio around 5 (720 nm ± 65 nm long) [14,25]. The comparison between spherical-shaped and rod-shaped MSNs showed that nanospheres were mostly excreted during the first few hours [25,165], while nanorods had slower clearance rates. In some studies, nearly intact MSNs were consistently found in the mice urine [14,25]. The content of silicon excreted in the feces was significantly higher than that detected in the urine [14,25,166].

The unique Cornell silica dots developed by the Wiesner group [167–170] received the American Food and Drug Administration (FDA) Investigational New Drug approval for first-in-human trials as a drug for targeted molecular imaging of integrin-expressing cancers. These multifunctional silica NPs were used in imaging tumor sites of five melanoma patients [14,167]. The silica NPs biodistribution and clearance were investigated and a rapid excretion was revealed: ~90% via kidneys and ~10% via the hepatobiliary route.

Despite several efforts and studies focused on the design of smart MSNs-based nanocarriers, evaluated by several administration routes,

their clinical translation is still scarce, and it remains a great challenge for most research groups concerned with therapy and diagnosis.

5. Benefits and challenges of MSNs as nanotherapeutics

The ideal biological behavior, good biocompatibility, biodegradability, and complete and short clearance time are the challenges of any nanostructure designed for therapeutic purposes. MSNs are widely investigated as nanocarriers due to several factors. The physicochemical parameters of the MSNs can be precisely tuned to achieve good behavior and effective drug loading and release at the desired site, comprising efficient nanoplatforms [4,171,172]. The scale of MSNs interactions with living systems is another factor. The MSNs allow good control over the pharmacokinetic profile of the transported therapeutic agent. The use of MSNs as controlled drug delivery systems could keep the drug concentration at optimal levels over prolonged periods of time, improving the treatment efficiency and avoiding any type of potential toxicity and the subsequent side effects. MSNs can also protect the therapeutic agents. The great loading capacity of MSNs favors the transport of two or more drugs into the same nanoparticles, which makes it possible to design combined therapies for tackling multi-resistant tumors. This feature allows the inclusion of certain contrast agents for biomedical imaging, which could be very interesting for following up on the treatment evolution in real-time [173,174].

On the other hand, MSNs face many unique challenges that need to be overcome in order to gain clinical approval and subsequently impact clinical healthcare [175]. MSNs clinical translation is still a great challenge requiring long-term stability and scale-up of these nanostructures, and it needs to pass the regulating authorities' evaluation [171,172,176]. The industrial technology transfer would depend on the scaling-up process, which together with the reproducibility and the total costs, constitutes the ordinary barriers for commercialization. The scaling-up of MSNs synthesis is not trivial because many different factors must be taken into account during the synthetic procedure [173,174]. The production of large-scale batches under Good Manufacturing Practices (GMP) conditions, needed for preclinical screening, clinical trials, and clinical use, is a roadblock for their commercialization. Reproducibility on the MSNs synthesis at a small scale is relatively easy, but at the larger and industrial scale, it is very difficult to control [173,177]. Another key point during the planning of the clinical trials should be dealing with regulatory agencies, such as the American FDA and the European Medicines Agency (EMA). Nowadays, there are no specific requirements for nanomedicines from these agencies, and the evaluation process follows the same path as that for small-molecule drugs. In the near future, the regulatory agencies are expected to develop specific requirements for nanomedicines to accelerate the translation from the lab to the clinic [152,173,177]. The potential challenge to the clinical translation of the MSN-based drug delivery system lies in the lack of substantial evidence on its chronic toxicity studies, genotoxicity and teratogenic potential, and long-term tissue compatibility. The degradation mechanism of mesoporous silica *in vivo* has not been well established yet. Efforts are to be made to bridge the gap between the preclinical and clinical use of MSNs and achieve marked progress in this subject [152].

6. Conclusions and perspectives

Most clinical therapies using drugs suffer from low bioavailability, specificity, and efficacy and show several side effects to healthy cells and tissues. Accordingly, several treatments based on drug-loaded nanocarriers have been proposed and designed to achieve good cost-effectiveness and FDA approval. In this context, MSNs have been widely exploited as interesting nanoplatforms to solve most of the drawbacks aforementioned, conferring tunable and remarkable properties such as high surface area, easy functionalization, high loading and release capacities, interesting pore and size structures, as well as low toxicity, high bioavailability, biodegradability, and clearance. However, to build an interesting and specific multifunctional MSNs-based nanocarrier, it is extremely important to know the exposure routes through which these nanosystems will reach the target site and, consequently, efficiently treat any disease. In light of this, the main exposure routes exploiting MSNs as efficient nanocarriers comprise intravenous, subcutaneous, intramuscular, intratumoral, ophthalmic, pulmonary, nasal, dermal, and oral administration. Most research groups have reported preclinical assays (*in vitro* and *in vivo* results) by using MSNs as nanoplatforms for drug delivery via all the mentioned administration routes. Notwithstanding, most studies reported to date have highlighted the use of intravenous, oral, and intratumoral administration as the main routes, with the evaluation of the multifunctional MSNs-based nanocarriers via ophthalmic, pulmonary, nasal, and dermal routes being very scarce. Therefore, the exponential growth of MSNs as nanoplatforms for efficient drug delivery and the few reports describing the possibilities of administration routes for MSNs, we believe that the understanding and better exploitation of all these administration routes in preclinical assays will contribute to developing smart MSNs-based nanocarriers with high stability in physiological media, specificity, and efficacy to treat most diseases, especially cancer. In addition, after a better understanding of the aforementioned implications and of the biodistribution, biodegradability, and clearance of these nanosystems, the complexity of the human body will be more thoroughly studied, thus opening interesting perspectives for clinical translations in the near future.

Declaration of competing interest

The authors declare that they have no known competing financial interests or personal relationships that could have appeared to influence the work reported in this paper.

Acknowledgments

The authors are grateful to the São Paulo Research Foundation – FAPESP (grant number #18/25377-3) for the research fellowship and financial support. This study is part of the National Institute of Science and Technology in Pharmaceutical Nanotechnology: a transdisciplinary approach INCT-NANOFARMA, which is supported by Sao Paulo Research Foundation (FAPESP, Brazil) Grant #2014/50928-2, and by "Conselho Nacional de Desenvolvimento Científico e Tecnológico" (CNPq, Brazil) Grant # 465687/2014-8.

References

[1] A.D. Maynard, R.J. Aitken, T. Butz, V. Colvin, K. Donaldson, G. Oberdörster, M. A. Philbert, J. Ryan, A. Seaton, V. Stone, S.S. Tinkle, L. Tran, N.J. Walker, D. B. Warheit, Safe handling of nanotechnology, Nature 444 (2006) 267–269, https://doi.org/10.1038/444267a.

[2] J. Bourquin, A. Milosevic, D. Hauser, R. Lehner, F. Blank, A. Petri-Fink, B. Rothen-Rutishauser, Biodistribution, clearance, and long-term fate of clinically relevant nanomaterials, Adv. Mater. 30 (2018) 1704307, https://doi.org/10.1002/adma.201704307.

[3] C. Murugan, V. Sharma, R.K. Murugan, G. Malaimegu, A. Sundaramurthy, Two-dimensional cancer theranostic nanomaterials: synthesis, surface functionalization and applications in photothermal therapy, J. Contr. Release 299 (2019) 1–20, https://doi.org/10.1016/j.jconrel.2019.02.015.

[4] R.M. Sábio, A.B. Meneguin, T.C. Ribeiro, R.R. Silva, M. Chorilli, New insights towards mesoporous silica nanoparticles as a technological platform for chemotherapeutic drugs delivery, Int. J. Pharm. 564 (2019) 379–409, https://doi.org/10.1016/j.ijpharm.2019.04.067.

[5] J. Chen, T. Fan, Z. Xie, Q. Zeng, P. Xue, T. Zheng, Y. Chen, X. Luo, H. Zhang, Advances in Nanomaterials for Photodynamic Therapy Applications: Status and Challenges, Biomaterials vol. 237 (2020) 119827, https://doi.org/10.1016/j.biomaterials.2020.119827.

[6] J. Majumder, O. Taratula, T. Minko, Nanocarrier-based systems for targeted and site specific therapeutic delivery, Adv. Drug Deliv. Rev. 144 (2019) 57–77, https://doi.org/10.1016/j.addr.2019.07.010.

[7] J. Lu, M. Liong, Z. Li, J.I. Zink, F. Tamanoi, Biocompatibility, biodistribution, and drug-delivery efficiency of mesoporous silica nanoparticles for cancer therapy in animals, Small 6 (2010) 1794–1805, https://doi.org/10.1002/smll.201000538.

[8] Z. Li, J.C. Barnes, A. Bosoy, J.F. Stoddart, J.I. Zink, Mesoporous silica nanoparticles in biomedical applications, Chem. Soc. Rev. 41 (2012) 2590–2605, https://doi.org/10.1039/c1cs15246g.
[9] T. Zhao, A. Elzatahry, X. Li, D. Zhao, Single-micelle-directed synthesis of mesoporous materials, Nat. Rev. Mater. 4 (2019) 775–791, https://doi.org/10.1038/s41578-019-0144-x.
[10] R.M. Sábio, S.H. Santagneli, M. Gressier, J.M.A. Caiut, W.M. Pazin, S.J.L. Ribeiro, M.-J. Menu, Near-infrared/visible-emitting nanosilica modified with silylated Ru (II) and Ln(III) complexes, Nanotechnology 31 (2020), 035602, https://doi.org/10.1088/1361-6528/ab494f.
[11] H. Omar, B. Moosa, K. Alamoudi, D.H. Anjum, A.H. Emwas, O. El Tall, B. Vu, F. Tamanoi, A. Almalik, N.M. Khashab, Impact of pore-walls ligand assembly on the biodegradation of mesoporous organosilica nanoparticles for controlled drug delivery, ACS Omega 3 (2018) 5195–5201, https://doi.org/10.1021/acsomega.8b00418.
[12] N. Hao, L. Li, Q. Zhang, X. Huang, X. Meng, Y. Zhang, D. Chen, F. Tang, L. Li, The shape effect of PEGylated mesoporous silica nanoparticles on cellular uptake pathway in Hela cells, Microporous Mesoporous Mater. 162 (2012) 14–23, https://doi.org/10.1016/j.micromeso.2012.05.040.
[13] N. Hao, L. Li, F. Tang, Shape-mediated biological effects of mesoporous silica nanoparticles, J. Biomed. Nanotechnol. 10 (2014) 2508–2538, https://doi.org/10.1166/jbn.2014.1940.
[14] J.G. Croissant, Y. Fatieiev, N.M. Khashab, Degradability and clearance of silicon, organosilica, silsesquioxane, silica mixed oxide, and mesoporous silica nanoparticles, Adv. Mater. 29 (2017) 1604634, https://doi.org/10.1002/adma.201604634.
[15] J. Zhang, H. Tang, Z. Liu, B. Chen, Effects of major parameters of nanoparticles on their physical and chemical properties and recent application of nanodrug delivery system in targeted chemotherapy, Int. J. Nanomed. 12 (2017) 8483–8493, https://doi.org/10.2147/IJN.S148359.
[16] K. Braun, C.M. Stürzel, J. Biskupek, U. Kaiser, F. Kirchhoff, M. Lindén, Comparison of different cytotoxicity assays for in vitro evaluation of mesoporous silica nanoparticles, Toxicol. Vitro 52 (2018) 214–221, https://doi.org/10.1016/j.tiv.2018.06.019.
[17] F. Lu, S.-H. Wu, Y. Hung, C.-Y. Mou, Size effect on cell uptake in well-suspended, uniform mesoporous silica nanoparticles, Small 5 (2009) 1408–1413, https://doi.org/10.1002/smll.200900005.
[18] F. Maturi, R. Sábio, R. Silva, M. Lahoud, A. Meneguin, G. Valente, R. Caface, I. Leite, N. Inada, S. Ribeiro, F.E. Maturi, R.M. Sábio, R.R. Silva, M.G. Lahoud, A. B. Meneguin, G.T. Valente, R.A. Caface, I.S. Leite, N.M. Inada, S.J.L. Ribeiro, Luminescent mesoporous silica nanohybrid based on drug derivative terbium complex, Materials 12 (2019) 933, https://doi.org/10.3390/ma12060933.
[19] R.M. Sábio, S.H. Santagneli, M. Gressier, J.M.A. Caiut, W.M. Pazin, I.S. Leite, N. M. Inada, R. Rosa da Silva, S.J.L. Ribeiro, M.-J. Menu, Luminescent nanohybrids based on silica and silylated Ru(II)—Yb(III) heterobinuclear complex: new tools for biological media analysis, Nanotechnology 31 (2020), 085709, https://doi.org/10.1088/1361-6528/ab55c3.
[20] D. Bhavsar, V. Patel, K. Sawant, Systematic investigation of in vitro and in vivo safety, toxicity and degradation of mesoporous silica nanoparticles synthesized using commercial sodium silicate, Microporous Mesoporous Mater. 284 (2019) 343–352, https://doi.org/10.1016/j.micromeso.2019.04.050.
[21] J. Ke, Y. Wang, L. Wang, B. Yang, K. Gou, Y. Qin, S. Li, H. Li, Synthesis and characterization of core-shell mesoporous silica nanoparticles with various shell thickness as indomethacin carriers: in vitro and in vivo evaluation, Microporous Mesoporous Mater. 297 (2020) 110043, https://doi.org/10.1016/j.micromeso.2020.110043.
[22] H. Wu, X. Wang, J. Zheng, L. Zhang, X. Li, W. Yuan, X. Liu, Propranolol-loaded mesoporous silica nanoparticles for treatment of infantile hemangiomas, Adv. Healthc. Mater. 8 (2019) 1801261, https://doi.org/10.1002/adhm.201801261.
[23] S. Vandghanooni, J. Barar, M. Eskandani, Y. Omidi, Aptamer-conjugated mesoporous silica nanoparticles for simultaneous imaging and therapy of cancer, TrAC Trends Anal. Chem. (Reference Ed.) 123 (2020) 115759, https://doi.org/10.1016/j.trac.2019.115759.
[24] J.-G. Sun, Q. Jiang, X.-P. Zhang, K. Shan, B.-H. Liu, C. Zhao, B. Yan, Mesoporous silica nanoparticles as a delivery system for improving antiangiogenic therapy, Int. J. Nanomed. 14 (2019) 1489–1501, https://doi.org/10.2147/IJN.S195504.
[25] J.G. Croissant, Y. Fatieiev, A. Almalik, N.M. Khashab, Mesoporous silica and organosilica nanoparticles: physical chemistry, biosafety, delivery strategies, and biomedical applications, Adv. Healthc. Mater. 7 (2018) 1700831, https://doi.org/10.1002/adhm.201700831.
[26] Y. Chen, H. Chen, J. Shi, In Vivo bio-safety evaluations and diagnostic/therapeutic applications of chemically designed mesoporous silica nanoparticles, Adv. Mater. 25 (2013) 3144–3176, https://doi.org/10.1002/adma.201205292.
[27] V. Balasubramanian, A. Domanskyi, J.-M. Renko, M. Sarparanta, C.-F. Wang, A. Correia, E. Mäkilä, O.S. Alanen, J. Salonen, A.J. Airaksinen, R. Tuominen, J. Hirvonen, M. Airavaara, H.A. Santos, Engineered antibody-functionalized porous silicon nanoparticles for therapeutic targeting of pro-survival pathway in endogenous neuroblasts after stroke, Biomaterials 227 (2020) 119556, https://doi.org/10.1016/j.biomaterials.2019.119556.
[28] B. Yang, Y. Chen, J. Shi, Mesoporous silica/organosilica nanoparticles: synthesis, biological effect and biomedical application, Mater. Sci. Eng. R Rep. 137 (2019) 66–105, https://doi.org/10.1016/j.mser.2019.01.001.
[29] K.S.W. Sing, Reporting physisorption data for gas/solid systems with special reference to the determination of surface area and porosity (Recommendations 1984), Pure Appl. Chem. 57 (1985) 603–619, https://doi.org/10.1351/pac198557040603.
[30] C.T. Kresge, M.E. Leonowicz, W.J. Roth, J.C. Vartuli, J.S. Beck, Ordered mesoporous molecular sieves synthesized by a liquid-crystal template mechanism, Nature 359 (1992) 710–712, https://doi.org/10.1038/359710a0.
[31] M. Grün, I. Lauer, K.K. Unger, The synthesis of micrometer- and submicrometer-size spheres of ordered mesoporous oxide MCM-41, Adv. Mater. 9 (1997) 254–257, https://doi.org/10.1002/adma.19970090317.
[32] C.E. Fowler, D. Khushalani, B. Lebeau, S. Mann, Nanoscale materials with mesostructured interiors, Adv. Mater. 13 (2001) 649–652, https://doi.org/10.1002/1521-4095(200105)13:9<649::AID-ADMA649>3.0.CO;2-G.
[33] W. Stöber, A. Fink, E. Bohn, Controlled growth of monodisperse silica spheres in the micron size range, J. Colloid Interface Sci. 26 (1968) 62–69, https://doi.org/10.1016/0021-9797(68)90272-5.
[34] V.-C. Niculescu, Mesoporous silica nanoparticles for bio-applications, Front. Mater. 7 (2020) 36, https://doi.org/10.3389/fmats.2020.00036.
[35] V. Valtchev, L. Tosheva, Porous nanosized particles: preparation, properties, and applications, Chem. Rev. 113 (2013) 6734–6760, https://doi.org/10.1021/cr300439k.
[36] F. Hoffmann, M. Cornelius, J. Morell, M. Fröba, Silica-based mesoporous organic–inorganic hybrid materials, Angew. Chem. Int. Ed. 45 (2006) 3216–3251, https://doi.org/10.1002/anie.200503075.
[37] Y. Wan, D. Zhao, On the controllable soft-templating approach to mesoporous silicates, Chem. Rev. 107 (2007) 2821–2860, https://doi.org/10.1021/cr068020s.
[38] A. Rahikkala, S.A.P. Pereira, P. Figueiredo, M.L.C. Passos, A.R.T.S. Araújo, M.L.M. F.S. Saraiva, H.A. Santos, Mesoporous silica nanoparticles for targeted and stimuli-responsive delivery of chemotherapeutics: a review, Adv. Biosyst. 2 (2018) 1800020, https://doi.org/10.1002/adbi.201800020.
[39] F. Chen, F. Zhang, D. Shao, W. Zhang, L. Zheng, W. Wang, W. Yang, Z. Wang, J. Chen, W. Dong, F. Xiao, Y. Wu, Bioreducible and traceable Ru(III) prodrug-loaded mesoporous silica nanoparticles for sequentially targeted nonsmall cell lung cancer chemotherapy, Appl. Mater. Today 19 (2020) 100558, https://doi.org/10.1016/j.apmt.2020.100558.
[40] D. Li, T. Zhang, C. Min, H. Huang, D. Tan, W. Gu, Biodegradable theranostic nanoplatforms of albumin-biomineralized nanocomposites modified hollow mesoporous organosilica for photoacoustic imaging guided tumor synergistic therapy, Chem. Eng. J. 388 (2020) 124253, https://doi.org/10.1016/j.cej.2020.124253.
[41] Y. Song, B. Zhou, X. Du, Y. Wang, J. Zhang, Y. Ai, Z. Xia, G. Zhao, Folic acid (FA)-conjugated mesoporous silica nanoparticles combined with MRP-1 siRNA improves the suppressive effects of myricetin on non-small cell lung cancer (NSCLC), Biomed. Pharmacother. 125 (2020) 109561, https://doi.org/10.1016/j.biopha.2019.109561.
[42] H. Lu, Q. Zhao, X. Wang, Y. Mao, C. Chen, Y. Gao, C. Sun, S. Wang, Multi-stimuli responsive mesoporous silica-coated carbon nanoparticles for chemo-photothermal therapy of tumor, Colloids Surf. B Biointerfaces 190 (2020) 110941, https://doi.org/10.1016/j.colsurfb.2020.110941.
[43] W. Lei, C. Sun, T. Jiang, Y. Gao, Y. Yang, Q. Zhao, S. Wang, Polydopamine-coated mesoporous silica nanoparticles for multi-responsive drug delivery and combined chemo-photothermal therapy, Mater. Sci. Eng. C 105 (2019) 110103, https://doi.org/10.1016/j.msec.2019.110103.
[44] X. Li, G. He, H. Jin, J. Tao, X. Li, C. Zhai, Y. Luo, X. Liu, Dual-Therapeutics-loaded mesoporous silica nanoparticles applied for breast tumor therapy, ACS Appl. Mater. Interfaces 11 (2019) 46497–46503, https://doi.org/10.1021/acsami.9b16270.
[45] J. Gao, K. Fan, Y. Jin, L. Zhao, Q. Wang, Y. Tang, H. Xu, Z. Liu, S. Wang, J. Lin, D. Lin, PEGylated lipid bilayer coated mesoporous silica nanoparticles co-delivery of paclitaxel and curcumin leads to increased tumor site drug accumulation and reduced tumor burden, Eur. J. Pharmaceut. Sci. 140 (2019) 105070, https://doi.org/10.1016/j.ejps.2019.105070.
[46] C.M. Liu, G.B. Chen, H.H. Chen, J. Bin Zhang, H.Z. Li, M.X. Sheng, W. Bin Weng, S.M. Guo, Cancer cell membrane-cloaked mesoporous silica nanoparticles with a pH-sensitive gatekeeper for cancer treatment, Colloids Surf. B Biointerfaces 175 (2019) 477–486, https://doi.org/10.1016/j.colsurfb.2018.12.038.
[47] D. Bhavsar, J. Gajjar, K. Sawant, Formulation and development of smart pH responsive mesoporous silica nanoparticles for breast cancer targeted delivery of anastrozole: in vitro and in vivo characterizations, Microporous Mesoporous Mater. 279 (2019) 107–116, https://doi.org/10.1016/j.micromeso.2018.12.026.
[48] J. Fang, Q. Wang, G. Yang, X. Xiao, L. Li, T. Yu, Albumin-MnO_2 gated hollow mesoporous silica nanosystem for modulating tumor hypoxia and synergetic therapy of cervical carcinoma, Colloids Surf. B Biointerfaces 179 (2019) 250–259, https://doi.org/10.1016/j.colsurfb.2019.03.070.
[49] D. Wang, Q. Zhao, T. Jiang, L. Sha, S. Wang, Y. Song, Large amino acid transporter 1 mediated glutamate modified mesoporous silica nanoparticles for chemophotothermal therapy, J. Drug Deliv. Sci. Technol. 52 (2019) 784–793, https://doi.org/10.1016/j.jddst.2019.05.043.
[50] L. Sha, Q. Zhao, D. Wang, X. Li, X. Wang, X. Guan, S. Wang, "Gate" engineered mesoporous silica nanoparticles for a double inhibition of drug efflux and particle exocytosis to enhance antitumor activity, J. Colloid Interface Sci. 535 (2019) 380–391, https://doi.org/10.1016/j.jcis.2018.09.089.
[51] S. Jiang, L. Hua, Z. Guo, L. Sun, One-pot green synthesis of doxorubicin loaded-silica nanoparticles for in vivo cancer therapy, Mater. Sci. Eng. C 90 (2018) 257–263, https://doi.org/10.1016/j.msec.2018.04.047.
[52] Z. Wang, Z. Chang, M. Lu, D. Shao, J. Yue, D. Yang, X. Zheng, M. Li, K. He, M. Zhang, L. Chen, W.-F. Dong, Shape-controlled magnetic mesoporous silica nanoparticles for magnetically-mediated suicide gene therapy of hepatocellular

carcinoma, Biomaterials 154 (2018) 147–157, https://doi.org/10.1016/j.biomaterials.2017.10.047.
[53] J. Zhao, P. Xie, C. Ye, C. Wu, W. Han, M. Huang, S. Wang, H. Chen, Outside-in synthesis of mesoporous silica/molybdenum disulfide nanoparticles for antitumor application, Chem. Eng. J. 351 (2018) 157–168, https://doi.org/10.1016/j.cej.2018.06.101.
[54] M. Nejabat, M. Mohammadi, K. Abnous, S.M. Taghdisi, M. Ramezani, M. Alibolandi, Fabrication of acetylated carboxymethylcellulose coated hollow mesoporous silica hybrid nanoparticles for nucleolin targeted delivery to colon adenocarcinoma, Carbohydr. Polym. (2018), https://doi.org/10.1016/j.carbpol.2018.05.092.
[55] L. Yu, Y. Chen, H. Lin, W. Du, H. Chen, J. Shi, Ultrasmall Mesoporous Organosilica Nanoparticles: Morphology Modulations and Redox-Responsive Biodegradability for Tumor-specific Drug Delivery, Biomaterials, 2018, https://doi.org/10.1016/j.biomaterials.2018.01.046.
[56] J.Y. Choi, B. Gupta, T. Ramasamy, J.H. Jeong, S.G. Jin, H.G. Choi, C.S. Yong, J. O. Kim, PEGylated polyaminoacid-capped mesoporous silica nanoparticles for mitochondria-targeted delivery of celastrol in solid tumors, Colloids Surfaces B Biointerfaces, 2018, https://doi.org/10.1016/j.colsurfb.2018.02.015.
[57] J. Wu, D.H. Bremner, S. Niu, H. Wu, J. Wu, H. Wang, H. Li, L.M. Zhu, Functionalized MoS_2 nanosheet-capped periodic mesoporous organosilicas as a multifunctional platform for synergistic targeted chemo-photothermal therapy, Chem. Eng. J. (2018), https://doi.org/10.1016/j.cej.2018.02.052.
[58] C. Xu, F. Chen, H.F. Valdovinos, D. Jiang, S. Goel, B. Yu, H. Sun, T.E. Barnhart, J. J. Moon, W. Cai, Bacteria-like mesoporous silica-coated gold nanorods for positron emission tomography and photoacoustic imaging-guided chemo-photothermal combined therapy, Biomaterials 165 (2018) 56–65, https://doi.org/10.1016/j.biomaterials.2018.02.043.
[59] P. Zhao, L. Li, S. Zhou, L. Qiu, Z. Qian, X. Liu, X. Cao, H. Zhang, TPGS functionalized mesoporous silica nanoparticles for anticancer drug delivery to overcome multidrug resistance, Mater. Sci. Eng. C 84 (2018) 108–117, https://doi.org/10.1016/j.msec.2017.11.040.
[60] M. Wu, H. Zhang, C. Tie, C. Yan, Z. Deng, Q. Wan, X. Liu, F. Yan, H. Zheng, MR imaging tracking of inflammation-activatable engineered neutrophils for targeted therapy of surgically treated glioma, Nat. Commun. 9 (2018) 4777, https://doi.org/10.1038/s41467-018-07250-6.
[61] N.S. Elbialy, S.F. Aboushoushah, B.F. Sofi, A. Noorwali, Multifunctional curcumin-loaded mesoporous silica nanoparticles for cancer chemoprevention and therapy, Microporous Mesoporous Mater. 291 (2020) 109540, https://doi.org/10.1016/j.micromeso.2019.06.002.
[62] T.L. Nguyen, B.G. Cha, Y. Choi, J. Im, J. Kim, Injectable dual-scale mesoporous silica cancer vaccine enabling efficient delivery of antigen/adjuvant-loaded nanoparticles to dendritic cells recruited in local macroporous scaffold, Biomaterials 239 (2020) 119859, https://doi.org/10.1016/j.biomaterials.2020.119859.
[63] L. Wang, X. Niu, Q. Song, J. Jia, Y. Hao, C. Zheng, K. Ding, H. Xiao, X. Liu, Z. Zhang, Y. Zhang, A two-step precise targeting nanoplatform for tumor therapy via the alkyl radicals activated by the microenvironment of organelles, J. Contr. Release 318 (2020) 197–209, https://doi.org/10.1016/j.jconrel.2019.10.017.
[64] Y. Zhang, J. Cheng, N. Li, R. Wang, G. Huang, J. Zhu, D. He, A versatile theranostic nanoplatform based on mesoporous silica, Mater. Sci. Eng. C 98 (2019) 560–571, https://doi.org/10.1016/j.msec.2019.01.004.
[65] M. Kovalainen, J. Mönkäre, M. Kaasalainen, J. Riikonen, V.-P. Lehto, J. Salonen, K.-H. Herzig, K. Järvinen, Development of porous silicon nanocarriers for parenteral peptide delivery, Mol. Pharm. 10 (2013) 353–359, https://doi.org/10.1021/mp300494p.
[66] D.L. Clemens, B.-Y. Lee, S. Plamthottam, M.V. Tullius, R. Wang, C.-J. Yu, Z. Li, B. J. Dillon, J.I. Zink, M.A. Horwitz, Nanoparticle formulation of moxifloxacin and intramuscular route of delivery improve antibiotic pharmacokinetics and treatment of pneumonic tularemia in a mouse model, ACS Infect. Dis. 5 (2019) 281–291, https://doi.org/10.1021/acsinfecdis.8b00268.
[67] S. Yang, J. Fan, S. Lin, Y. Wang, C. Liu, Novel pH-responsive biodegradable organosilica nanoparticles as drug delivery system for cancer therapy, Colloids Surfaces A Physicochem. Eng. Asp. 585 (2020) 124133, https://doi.org/10.1016/j.colsurfa.2019.124133.
[68] L. Xing, X. Li, Z. Xing, F. Li, M. Shen, H. Wang, X. Shi, L. Du, Silica/gold nanoplatform combined with a thermosensitive gel for imaging-guided interventional therapy in PDX of pancreatic cancer, Chem. Eng. J. 382 (2020) 122949, https://doi.org/10.1016/j.cej.2019.122949.
[69] J. Zhou, M. Wang, Y. Han, J. Lai, J. Chen, Multistage-targeted gold/mesoporous silica nanocomposite hydrogel as in situ injectable drug release system for chemophotothermal synergistic cancer therapy, ACS Appl. Bio Mater. 3 (2020) 421–431, https://doi.org/10.1021/acsabm.9b00895.
[70] H. Wu, X. Wang, H. Liang, J. Zheng, S. Huang, D. Zhang, Enhanced efficacy of propranolol therapy for infantile hemangiomas based on a mesoporous silica nanoplatform through mediating autophagy dysfunction, Acta Biomater. 107 (2020) 272–285, https://doi.org/10.1016/j.actbio.2020.02.033.
[71] M. Gautam, R.K. Thapa, B.K. Poudel, B. Gupta, H.B. Ruttala, H.T. Nguyen, Z. C. Soe, W. Ou, K. Poudel, H.G. Choi, S.K. Ku, C.S. Yong, J.O. Kim, Aerosol technique-based carbon-encapsulated hollow mesoporous silica nanoparticles for synergistic chemo-photothermal therapy, Acta Biomater. 88 (2019) 448–461, https://doi.org/10.1016/j.actbio.2019.02.029.
[72] N. Lu, P. Huang, W. Fan, Z. Wang, Y. Liu, S. Wang, G. Zhang, J. Hu, W. Liu, G. Niu, R.D. Leapman, G. Lu, X. Chen, Tri-stimuli-responsive biodegradable theranostics for mild hyperthermia enhanced chemotherapy, Biomaterials 126 (2017) 39–48, https://doi.org/10.1016/j.biomaterials.2017.02.025.
[73] C. Liu, Y. Zhang, M. Liu, Z. Chen, Y. Lin, W. Li, F. Cao, Z. Liu, J. Ren, X. Qu, A NIR-controlled cage mimicking system for hydrophobic drug mediated cancer therapy, Biomaterials 139 (2017) 151–162, https://doi.org/10.1016/j.biomaterials.2017.06.008.
[74] K. Dong, Z. Li, H. Sun, E. Ju, J. Ren, X. Qu, Pathogen-mimicking nanocomplexes: self-stimulating oxidative stress in tumor microenvironment for chemo-immunotherapy, Mater, Today Off. 20 (2017) 346–353, https://doi.org/10.1016/j.mattod.2017.06.003.
[75] S.-N. Kim, S.A. Ko, C.G. Park, S.H. Lee, B.K. Huh, Y.H. Park, Y.K. Kim, A. Ha, K. H. Park, Y. Bin Choy, Amino-functionalized mesoporous silica particles for ocular delivery of brimonidine, Mol. Pharm. 15 (2018) 3143–3152, https://doi.org/10.1021/acs.molpharmaceut.8b00215.
[76] S. Lungare, K. Hallam, R.K.S. Badhan, Phytochemical-loaded mesoporous silica nanoparticles for nose-to-brain olfactory drug delivery, Int. J. Pharm. 513 (2016) 280–293, https://doi.org/10.1016/j.ijpharm.2016.09.042.
[77] Y. Shen, B. Cao, N.R. Snyder, K.M. Woeppel, J.R. Eles, X.T. Cui, ROS responsive resveratrol delivery from LDLR peptide conjugated PLA-coated mesoporous silica nanoparticles across the blood–brain barrier, J. Nanobiotechnol. 16 (2018) 13, https://doi.org/10.1186/s12951-018-0340-7.
[78] Y. You, L. Yang, L. He, T. Chen, Tailored mesoporous silica nanosystem with enhanced permeability of the blood–brain barrier to antagonize glioblastoma, J. Mater. Chem. B. 4 (2016) 5980–5990, https://doi.org/10.1039/C6TB01329E.
[79] J. Mo, L. He, B. Ma, T. Chen, Tailoring particle size of mesoporous silica nanosystem to antagonize glioblastoma and overcome blood–brain barrier, ACS Appl. Mater. Interfaces 8 (2016) 6811–6825, https://doi.org/10.1021/acsami.5b11730.
[80] G.B. Heggannavar, S. Vijeth, M.Y. Kariduraganavar, Development of dual drug loaded PLGA based mesoporous silica nanoparticles and their conjugation with Angiopep-2 to treat glioma, J. Drug Deliv. Sci. Technol. 53 (2019) 101157, https://doi.org/10.1016/j.jddst.2019.101157.
[81] P. Zhang, M. Tang, Q. Huang, G. Zhao, N. Huang, X. Zhang, Y. Tan, Y. Cheng, Combination of 3-methyladenine therapy and Asn-Gly-Arg (NGR)-modified mesoporous silica nanoparticles loaded with temozolomide for glioma therapy in vitro, Biochem. Biophys. Res. Commun. 509 (2019) 549–556, https://doi.org/10.1016/j.bbrc.2018.12.158.
[82] J. Geng, M. Li, L. Wu, C. Chen, X. Qu, Mesoporous silica nanoparticle-based H_2O_2 responsive controlled-release system used for Alzheimer's disease treatment, Adv. Healthc. Mater. 1 (2012) 332–336, https://doi.org/10.1002/adhm.201200067.
[83] L. Yang, T. Yin, Y. Liu, J. Sun, Y. Zhou, J. Liu, Gold nanoparticle-capped mesoporous silica-based H_2O_2-responsive controlled release system for Alzheimer's disease treatment, Acta Biomater. 46 (2016) 177–190, https://doi.org/10.1016/j.actbio.2016.09.010.
[84] O. Taratula, O.B. Garbuzenko, A.M. Chen, T. Minko, Innovative strategy for treatment of lung cancer: targeted nanotechnology-based inhalation co-delivery of anticancer drugs and siRNA, J. Drug Target. 19 (2011) 900–914, https://doi.org/10.3109/1061186X.2011.622404.
[85] X. Li, M. Xue, O.G. Raabe, H.L. Aaron, E.A. Eisen, J.E. Evans, F.A. Hayes, S. Inaga, A. Tagmount, M. Takeuchi, C. Vulpe, J.I. Zink, S.H. Risbud, K.E. Pinkerton, Aerosol droplet delivery of mesoporous silica nanoparticles: a strategy for respiratory-based therapeutics, Nanomed. Nanotechnol. Biol. Med. 11 (2015) 1377–1385, https://doi.org/10.1016/j.nano.2015.03.007.
[86] E. Ugazio, L. Gastaldi, V. Brunella, D. Scalarone, S.A. Jadhav, S. Oliaro-Bosso, D. Zonari, G. Berlier, I. Miletto, S. Sapino, Thermoresponsive mesoporous silica nanoparticles as a carrier for skin delivery of quercetin, Int. J. Pharm. 511 (2016) 446–454, https://doi.org/10.1016/j.ijpharm.2016.07.024.
[87] S. Sapino, S. Oliaro-Bosso, D. Zonari, A. Zattoni, E. Ugazio, Mesoporous silica nanoparticles as a promising skin delivery system for methotrexate, Int. J. Pharm. 530 (2017) 239–248, https://doi.org/10.1016/j.ijpharm.2017.07.058.
[88] X. Ma, Q. Qu, Y. Zhao, Targeted delivery of 5-aminolevulinic acid by multifunctional hollow mesoporous silica nanoparticles for photodynamic skin cancer therapy, ACS Appl. Mater. Interfaces 7 (2015) 10671–10676, https://doi.org/10.1021/acsami.5b03087.
[89] D.C.S. Lio, C. Liu, M.M.S. Oo, C. Wiraja, M.H.Y. Teo, M. Zheng, S.W.T. Chew, X. Wang, C. Xu, Transdermal delivery of small interfering RNAs with topically applied mesoporous silica nanoparticles for facile skin cancer treatment, Nanoscale 11 (2019) 17041–17051, https://doi.org/10.1039/C9NR06303J.
[90] S. Nafisi, N. Samadi, M. Houshiar, H.I. Maibach, Mesoporous silica nanoparticles for enhanced lidocaine skin delivery, Int. J. Pharm. 550 (2018) 325–332, https://doi.org/10.1016/j.ijpharm.2018.08.004.
[91] N.Ž. Knežević, N. Ilić, V. Đokić, R. Petrović, D. Janaćković, Mesoporous silica and organosilica nanomaterials as UV-blocking agents, ACS Appl. Mater. Interfaces 10 (2018) 20231–20236, https://doi.org/10.1021/acsami.8b04635.
[92] S.H. Tolbert, P.D. McFadden, D.A. Loy, New hybrid organic/inorganic polysilsesquioxane-silica particles as sunscreens, ACS Appl. Mater. Interfaces 8 (2016) 3160–3174, https://doi.org/10.1021/acsami.5b10472.
[93] R. Ebabe Elle, S. Rahmani, C. Lauret, M. Morena, L.P.R. Bidel, A. Boulahtouf, P. Balaguer, J.-P. Cristol, J.-O. Durand, C. Charnay, E. Badia, Functionalized mesoporous silica nanoparticle with antioxidants as a new carrier that generates lower oxidative stress impact on cells, Mol. Pharm. 13 (2016) 2647–2660, https://doi.org/10.1021/acs.molpharmaceut.6b00190.
[94] X. Li, C.-H. Wong, T.-W. Ng, C.-F. Zhang, K.C.-F. Leung, L. Jin, The spherical nanoparticle-encapsulated chlorhexidine enhances anti-biofilm efficiency through an effective releasing mode and close microbial interactions, Int. J. Nanomed. 11 (2016) 2471, https://doi.org/10.2147/IJN.S105681.
[95] T.S. Anirudhan, A.S. Nair, Temperature and ultrasound sensitive gatekeepers for the controlled release of chemotherapeutic drugs from mesoporous silica

nanoparticles, J. Mater. Chem. B. 6 (2018) 428–439, https://doi.org/10.1039/C7TB02292A.
[96] W. Zhang, N. Zheng, L. Chen, L. Xie, M. Cui, S. Li, L. Xu, Effect of shape on mesoporous silica nanoparticles for oral delivery of indomethacin, Pharmaceutics 11 (2018) 4, https://doi.org/10.3390/pharmaceutics11010004.
[97] S.B. Hartono, L. Hadisoewignyo, Y. Yang, A.K. Meka, C. Yu Antaresti, Amine functionalized cubic mesoporous silica nanoparticles as an oral delivery system for curcumin bioavailability enhancement, Nanotechnology 27 (2016) 505605, https://doi.org/10.1088/0957-4484/27/50/505605.
[98] Y. Gao, S. Ding, X. Huang, Z. Fan, J. Sun, Y. Hai, K. Li, Development and evaluation of hollow mesoporous silica microspheres bearing on enhanced oral delivery of curcumin, Drug Dev. Ind. Pharm. 45 (2019) 273–281, https://doi.org/10.1080/03639045.2018.1539098.
[99] Y. Zhang, J. Wang, X. Bai, T. Jiang, Q. Zhang, S. Wang, Mesoporous silica nanoparticles for increasing the oral bioavailability and permeation of poorly water soluble drugs, Mol. Pharm. 9 (2012) 505–513, https://doi.org/10.1021/mp200287c.
[100] A. Karimi Bavandpour, B. Bakhshi, S. Najar-peerayeh, The roles of mesoporous silica and carbon nanoparticles in antigen stability and intensity of immune response against recombinant subunit B of cholera toxin in a rabbit animal model, Int. J. Pharm. 573 (2020) 118868, https://doi.org/10.1016/j.ijpharm.2019.118868.
[101] L. Li, T. Liu, C. Fu, L. Tan, X. Meng, H. Liu, Biodistribution, excretion, and toxicity of mesoporous silica nanoparticles after oral administration depend on their shape, Nanomed. Nanotechnol. Biol. Med. 11 (2015) 1915–1924, https://doi.org/10.1016/j.nano.2015.07.004.
[102] A. Guha, N. Biswas, K. Bhattacharjee, N. Sahoo, K. Kuotsu, pH responsive cylindrical MSN for oral delivery of insulin-design, fabrication and evaluation, Drug Deliv. 23 (2016) 3552–3561, https://doi.org/10.1080/10717544.2016.1209796.
[103] R.J. Mudakavi, A.M. Raichur, D. Chakravortty, Lipid coated mesoporous silica nanoparticles as an oral delivery system for targeting and treatment of intravacuolar Salmonella infections, RSC Adv. 4 (2014) 61160–61166, https://doi.org/10.1039/C4RA12973C.
[104] Y. Guo, L. Wu, K. Gou, Y. Wang, B. Hu, Y. Pang, S. Li, H. Li, Functional mesoporous silica nanoparticles for delivering nimesulide with chiral recognition performance, Microporous Mesoporous Mater. 294 (2020) 109862, https://doi.org/10.1016/j.micromeso.2019.109862.
[105] D. Chenthamara, S. Subramaniam, S.G. Ramakrishnan, S. Krishnaswamy, M. M. Essa, F.-H. Lin, M.W. Qoronfleh, Therapeutic efficacy of nanoparticles and routes of administration, Biomater. Res. 23 (2019) 20, https://doi.org/10.1186/s40824-019-0166-x.
[106] S.E. Parker, P.G. Davey, Pharmacoeconomics of intravenous drug administration, Pharmacoeconomics 1 (1992) 103–115, https://doi.org/10.2165/00019053-199201020-00007.
[107] M.A. Saxen, Pharmacologic management of patient behavior. McDonald Avery's Dent. Child Adolesc., Elsevier, 2016, pp. 303–327, https://doi.org/10.1016/B978-0-323-28745-6.00017-X.
[108] B. Bittner, W. Richter, J. Schmidt, Subcutaneous Administration of biotherapeutics: an overview of current challenges and opportunities, BioDrugs 32 (2018) 425–440, https://doi.org/10.1007/s40259-018-0295-0.
[109] A. Obinu, E. Gavini, G. Rassu, M. Maestri, M.C. Bonferoni, P. Giunchedi, Nanoparticles in detection and treatment of lymph node metastases: an update from the point of view of administration routes, Expet Opin. Drug Deliv. 15 (2018) 1117–1126, https://doi.org/10.1080/17425247.2018.1537260.
[110] J.E. Maddison, S.W. Page, T.M. Dyke, Clinical pharmacokinetics. Small Anim. Clin. Pharmacol., Elsevier, 2008, pp. 27–40, https://doi.org/10.1016/B978-070202858-8.50004-X.
[111] K.K. Jain, An overview of drug delivery systems. Methods Mol. Biol., Humana Press Inc., 2020, pp. 1–54, https://doi.org/10.1007/978-1-4939-9798-5_1.
[112] C. Fu, T. Liu, L. Li, H. Liu, D. Chen, F. Tang, The absorption, distribution, excretion and toxicity of mesoporous silica nanoparticles in mice following different exposure routes, Biomaterials 34 (2013) 2565–2575, https://doi.org/10.1016/j.biomaterials.2012.12.043.
[113] I. Brigger, C. Dubernet, P. Couvreur, Nanoparticles in cancer therapy and diagnosis, Adv. Drug Deliv. Rev. 64 (2012) 24–36, https://doi.org/10.1016/j.addr.2012.09.006.
[114] E. Dinte, O. Vostinaru, O. Samoila, B. Sevastre, E. Bodoki, Ophthalmic nanosystems with antioxidants for the prevention and treatment of eye diseases, Coatings 10 (2020) 36, https://doi.org/10.3390/coatings10010036.
[115] T.A.A. Ahmed, K.M. El-Say, O.A.A. Ahmed, A.S. Zidan, Sterile dosage forms loaded nanosystems for parenteral, nasal, pulmonary and ocular administration. Nanoscale Fabr. Optim. Scale-Up Biol. Asp. Pharm. Nanotechnol., Elsevier, 2018, pp. 335–395, https://doi.org/10.1016/B978-0-12-813629-4.00009-7.
[116] A. Kuzmov, T. Minko, Nanotechnology approaches for inhalation treatment of lung diseases, J. Contr. Release 219 (2015) 500–518, https://doi.org/10.1016/j.jconrel.2015.07.024.
[117] T. Wang, Y. Liu, C. Wu, Effect of paclitaxel-mesoporous silica nanoparticles with a core-shell structure on the human lung cancer cell line A549, Nanoscale Res. Lett. 12 (2017) 66, https://doi.org/10.1186/s11671-017-1826-1.
[118] M. Agrawal, S. Saraf, S. Saraf, S.G. Antimisiaris, M.B. Chougule, S.A. Shoyele, A. Alexander, Nose-to-brain drug delivery: an update on clinical challenges and progress towards approval of anti-Alzheimer drugs, J. Contr. Release 281 (2018) 139–177, https://doi.org/10.1016/j.jconrel.2018.05.011.
[119] A.R. Khan, M. Liu, M.W. Khan, G. Zhai, Progress in brain targeting drug delivery system by nasal route, J. Contr. Release 268 (2017) 364–389, https://doi.org/10.1016/j.jconrel.2017.09.001.
[120] L. Illum, I. Jabbal-Gill, M. Hinchcliffe, A.N. Fisher, S.S. Davis, Chitosan as a novel nasal delivery system for vaccines, Adv. Drug Deliv. Rev. 51 (2001) 81–96, https://doi.org/10.1016/S0169-409X(01)00171-5.
[121] S. Nafisi, M. Schäfer-Korting, H.I. Maibach, Perspectives on percutaneous penetration: silica nanoparticles, Nanotoxicology 9 (2015) 643–657, https://doi.org/10.3109/17435390.2014.958115.
[122] C. Vitorino, J. Sousa, A. Pais, Overcoming the skin permeation barrier: challenges and opportunities, Curr. Pharmaceut. Des. 21 (2015) 2698–2712, https://doi.org/10.2174/1381612821666150428124053.
[123] B. Fonseca-Santos, P.B. Silva, R.B. Rigon, M.R. Sato, M. Chorilli, Formulating SLN and NLC as innovative drug delivery systems for non-invasive routes of drug administration, Curr. Med. Chem. (2019), https://doi.org/10.2174/0929867326666190624155938.
[124] Y. Dancik, P.L. Bigliardi, M. Bigliardi-Qi, What happens in the skin? Integrating skin permeation kinetics into studies of developmental and reproductive toxicity following topical exposure, Reprod. Toxicol. 58 (2015) 252–281, https://doi.org/10.1016/j.reprotox.2015.10.001.
[125] R.J. Scheuplein, Mechanism of percutaneous absorption, J. Invest. Dermatol. 48 (1967) 79–88, https://doi.org/10.1038/jid.1967.11.
[126] F. Larese Filon, M. Mauro, G. Adami, M. Bovenzi, M. Crosera, Nanoparticles skin absorption: new aspects for a safety profile evaluation, Regul. Toxicol. Pharmacol. 72 (2015) 310–322, https://doi.org/10.1016/j.yrtph.2015.05.005.
[127] B.W. Barry, Novel mechanisms and devices to enable successful transdermal drug delivery, Eur. J. Pharmaceut. Sci. 14 (2001) 101–114, https://doi.org/10.1016/S0928-0987(01)00167-1.
[128] F. Erdő, N. Hashimoto, G. Karvaly, N. Nakamichi, Y. Kato, Critical evaluation and methodological positioning of the transdermal microdialysis technique, Rev. J. Contr. Releas. 233 (2016) 147–161, https://doi.org/10.1016/j.jconrel.2016.05.035.
[129] H.C. Korting, M. Schäfer-Korting, Carriers in the topical treatment of skin disease. Handb. Exp. Pharmacol., Springer, Berlin, Heidelberg, 2010, pp. 435–468, https://doi.org/10.1007/978-3-642-00477-3_15.
[130] A. Nigro, M. Pellegrino, M. Greco, A. Comandè, D. Sisci, L. Pasqua, A. Leggio, C. Morelli, Dealing with skin and blood-brain barriers: the unconventional challenges of mesoporous silica nanoparticles, Pharmaceutics 10 (2018) 250, https://doi.org/10.3390/pharmaceutics10040250.
[131] S. Sapino, E. Ugazio, L. Gastaldi, I. Miletto, G. Berlier, D. Zonari, S. Oliaro-Bosso, Mesoporous silica as topical nanocarriers for quercetin: characterization and in vitro studies, Eur. J. Pharm. Biopharm. 89 (2015) 116–125, https://doi.org/10.1016/j.ejpb.2014.11.022.
[132] P. Scodeller, P.N. Catalano, N. Salguero, H. Duran, A. Wolosiuk, G.J.A.A. Soler-Illia, Hyaluronan degrading silica nanoparticles for skin cancer therapy, Nanoscale 5 (2013) 9690, https://doi.org/10.1039/c3nr02787b.
[133] M.R. Prausnitz, P.M. Elias, T.J. Franz, M. Schmuth, J.-C. Tsai, G.K. Menon, W. M. Holleran, K.R. Feingold, Skin Barrier and Transdermal Drug Delivery, 2012.
[134] D.J. Bharali, I. Klejbor, E.K. Stachowiak, P. Dutta, I. Roy, N. Kaur, E.J. Bergey, P. N. Prasad, M.K. Stachowiak, Organically modified silica nanoparticles: a nonviral vector for in vivo gene delivery and expression in the brain, Proc. Natl. Acad. Sci. Unit. States Am. 102 (2005) 11539–11544, https://doi.org/10.1073/pnas.0504926102.
[135] P.P. Desai, A.A. Date, V.B. Patravale, Overcoming poor oral bioavailability using nanoparticle formulations – opportunities and limitations, Drug Discov. Today Technol. 9 (2012) e87–e95, https://doi.org/10.1016/j.ddtec.2011.12.001.
[136] Y. Yun, Y.W. Cho, K. Park, Nanoparticles for oral delivery: targeted nanoparticles with peptidic ligands for oral protein delivery, Adv. Drug Deliv. Rev. 65 (2013) 822–832, https://doi.org/10.1016/j.addr.2012.10.007.
[137] J. Florek, R. Caillard, F. Kleitz, Evaluation of mesoporous silica nanoparticles for oral drug delivery – current status and perspective of MSNs drug carriers, Nanoscale 9 (2017) 15252–15277, https://doi.org/10.1039/C7NR05762H.
[138] J.B. Dressman, H. Lennernäs, Oral Drug Absorption: Prediction and Assessment, Marcel Dekker, New York, 2000.
[139] A. Maroni, M.D. Del Curto, L. Zema, A. Foppoli, A. Gazzaniga, Film coatings for oral colon delivery, Int. J. Pharm. 457 (2013) 372–394, https://doi.org/10.1016/j.ijpharm.2013.05.043.
[140] A.C. Freire, A.W. Basit, R. Choudhary, C.W. Piong, H.A. Merchant, Does sex matter? The influence of gender on gastrointestinal physiology and drug delivery, Int. J. Pharm. 415 (2011) 15–28, https://doi.org/10.1016/j.ijpharm.2011.04.069.
[141] E. Roger, F. Lagarce, E. Garcion, J.-P. Benoit, Biopharmaceutical parameters to consider in order to alter the fate of nanocarriers after oral delivery, Nanomedicine 5 (2010) 287–306, https://doi.org/10.2217/nnm.09.110.
[142] C.A. Lipinski, F. Lombardo, B.W. Dominy, P.J. Feeney, Experimental and computational approaches to estimate solubility and permeability in drug discovery and development settings [1], Adv. Drug Deliv. Rev. 46 (2001) 3–26, https://doi.org/10.1016/S0169-409X(00)00129-0.
[143] J. Renukuntla, A.D. Vadlapudi, A. Patel, S.H.S. Boddu, A.K. Mitra, Approaches for enhancing oral bioavailability of peptides and proteins, Int. J. Pharm. 447 (2013) 75–93, https://doi.org/10.1016/j.ijpharm.2013.02.030.
[144] A.A. Date, N. Desai, R. Dixit, M. Nagarsenker, Self-nanoemulsifying drug delivery systems: formulation insights, applications and advances, Nanomedicine 5 (2010) 1595–1616, https://doi.org/10.2217/nnm.10.126.

[145] K. Thanki, R.P. Gangwal, A.T. Sangamwar, S. Jain, Oral delivery of anticancer drugs: challenges and opportunities, J. Contr. Release 170 (2013) 15–40, https://doi.org/10.1016/j.jconrel.2013.04.020.
[146] J.H. Hamman, G.M. Enslin, A.F. Kotzé, Oral delivery of peptide drugs, BioDrugs 19 (2005) 165–177, https://doi.org/10.2165/00063030-200519030-00003.
[147] R.I. Mahato, A.S. Narang, L. Thoma, D.D. Miller, Emerging trends in oral delivery of peptide and protein drugs, Crit. Rev. Ther. Drug Carrier Syst. 20 (2003) 153–214, https://doi.org/10.1615/CritRevTherDrugCarrierSyst.v20.i23.30.
[148] M. Sharma, R. Sharma, D.K. Jain, Nanotechnology based approaches for enhancing oral bioavailability of poorly water soluble antihypertensive drugs, Sci. Tech. Rep. (2016) (2016) 1–11, https://doi.org/10.1155/2016/8525679.
[149] C.T.H. Nguyen, R.I. Webb, L.K. Lambert, E. Strounina, E.C. Lee, M.-O. Parat, M. A. McGuckin, A. Popat, P.J. Cabot, B.P. Ross, Bifunctional succinylated ε-polylysine-coated mesoporous silica nanoparticles for pH-responsive and intracellular drug delivery targeting the colon, ACS Appl. Mater. Interfaces 9 (2017) 9470–9483, https://doi.org/10.1021/acsami.7b00411.
[150] X. Zhao, C. Shan, Y. Zu, Y. Zhang, W. Wang, K. Wang, X. Sui, R. Li, Preparation, characterization, and evaluation in vivo of Ins-SiO_2-HP55 (insulin-loaded silica coating HP55) for oral delivery of insulin, Int. J. Pharm. 454 (2013) 278–284, https://doi.org/10.1016/j.ijpharm.2013.06.051.
[151] L. Hadisoewignyo, S.B. Hartono, A. Kresnamurti, I. Soeliono, Y. Nataline, G. A. Prakoso, D.A.R.E. Aulia, Evaluation of anti-inflammatory activity and biocompatibility of curcumin loaded mesoporous silica nanoparticles as an oral drug delivery system, Adv. Nat. Sci. Nanosci. Nanotechnol. 9 (2018), 035007, https://doi.org/10.1088/2043-6254/aad5d5.
[152] R. Narayan, U. Nayak, A. Raichur, S. Garg, Mesoporous silica nanoparticles: a comprehensive review on synthesis and recent advances, Pharmaceutics 10 (2018) 118, https://doi.org/10.3390/pharmaceutics10030118.
[153] I.I. Slowing, C.-W. Wu, J.L. Vivero-Escoto, V.S.-Y. Lin, Mesoporous silica nanoparticles for reducing hemolytic activity towards mammalian red blood cells, Small 5 (2009) 57–62, https://doi.org/10.1002/smll.200800926.
[154] Q. He, Z. Zhang, F. Gao, Y. Li, J. Shi, In vivo biodistribution and urinary excretion of mesoporous silica nanoparticles: effects of particle size and PEGylation, Small 7 (2011) 271–280, https://doi.org/10.1002/smll.201001459.
[155] T. Yu, A. Malugin, H. Ghandehari, Impact of silica nanoparticle design on cellular toxicity and hemolytic activity, ACS Nano 5 (2011) 5717–5728, https://doi.org/10.1021/nn2013904.
[156] Q. Zhang, X. Wang, P.-Z. Li, K.T. Nguyen, X.-J. Wang, Z. Luo, H. Zhang, N.S. Tan, Y. Zhao, Biocompatible, uniform, and redispersible mesoporous silica nanoparticles for cancer-targeted drug delivery in vivo, Adv. Funct. Mater. 24 (2014) 2450–2461, https://doi.org/10.1002/adfm.201302988.
[157] G. Chen, Z. Teng, X. Su, Y. Liu, G. Lu, Unique biological degradation behavior of stöber mesoporous silica nanoparticles from their interiors to their exteriors, J. Biomed. Nanotechnol. 11 (2015) 722–729, https://doi.org/10.1166/jbn.2015.2072.
[158] Q. He, J. Shi, M. Zhu, Y. Chen, F. Chen, The three-stage in vitro degradation behavior of mesoporous silica in simulated body fluid, Microporous Mesoporous Mater. 131 (2010) 314–320, https://doi.org/10.1016/j.micromeso.2010.01.009.
[159] N. Hao, H. Liu, L. Li, D. Chen, L. Li, F. Tang, In Vitro degradation behavior of silica nanoparticles under physiological conditions, J. Nanosci. Nanotechnol. 12 (2012) 6346–6354, https://doi.org/10.1166/jnn.2012.6199.
[160] X. Huang, L. Li, T. Liu, N. Hao, H. Liu, D. Chen, F. Tang, The shape effect of mesoporous silica nanoparticles on biodistribution, clearance, and biocompatibility in vivo, ACS Nano 5 (2011) 5390–5399, https://doi.org/10.1021/nn200365a.
[161] R. Kumar, I. Roy, T.Y. Ohulchanskky, L.A. Vathy, E.J. Bergey, M. Sajjad, P. N. Prasad, In Vivo biodistribution and clearance studies using multimodal organically modified silica nanoparticles, ACS Nano 4 (2010) 699–708, https://doi.org/10.1021/nn901146y.
[162] M. Cho, W.-S. Cho, M. Choi, S.J. Kim, B.S. Han, S.H. Kim, H.O. Kim, Y.Y. Sheen, J. Jeong, The impact of size on tissue distribution and elimination by single intravenous injection of silica nanoparticles, Toxicol. Lett. 189 (2009) 177–183, https://doi.org/10.1016/j.toxlet.2009.04.017.
[163] X. He, H. Nie, K. Wang, W. Tan, X. Wu, P. Zhang, In Vivo study of biodistribution and urinary excretion of surface-modified silica nanoparticles, Anal. Chem. 80 (2008) 9597–9603, https://doi.org/10.1021/ac801882g.
[164] J.S. Souris, C.-H. Lee, S.-H. Cheng, C.-T. Chen, C.-S. Yang, J.A. Ho, C.-Y. Mou, L.-W. Lo, Surface charge-mediated rapid hepatobiliary excretion of mesoporous silica nanoparticles, Biomaterials 31 (2010) 5564–5574, https://doi.org/10.1016/j.biomaterials.2010.03.048.
[165] P.J. Kempen, S. Greasley, K.A. Parker, J.C. Campbell, H.-Y. Chang, J.R. Jones, R. Sinclair, S.S. Gambhir, J.V. Jokerst, Theranostic mesoporous silica nanoparticles biodegrade after pro-survival drug delivery and ultrasound/magnetic resonance imaging of stem cells, Theranostics 5 (2015) 631–642, https://doi.org/10.7150/thno.11389.
[166] Y.-L. Sun, Y. Zhou, Q.-L. Li, Y.-W. Yang, Enzyme-responsive supramolecular nanovalves crafted by mesoporous silica nanoparticles and choline-sulfonatocalix [4]arene [2]pseudorotaxanes for controlled cargo release, Chem. Commun. 49 (2013) 9033, https://doi.org/10.1039/c3cc45216f.
[167] M. Benezra, O. Penate-Medina, P.B. Zanzonico, D. Schaer, H. Ow, A. Burns, E. DeStanchina, V. Longo, E. Herz, S. Iyer, J. Wolchok, S.M. Larson, U. Wiesner, M.S. Bradbury, Multimodal silica nanoparticles are effective cancer-targeted probes in a model of human melanoma, J. Clin. Invest. 121 (2011) 2768–2780, https://doi.org/10.1172/JCI45600.
[168] M.S. Bradbury, M. Pauliah, P. Zanzonico, U. Wiesner, S. Patel, Intraoperative mapping of sentinel lymph node metastases using a clinically translated ultrasmall silica nanoparticle, Wiley Interdiscip. Rev. Nanomed. Nanobiotechnol. 8 (2016) 535–553, https://doi.org/10.1002/wnan.1380.
[169] M.S. Bradbury, E. Phillips, P.H. Montero, S.M. Cheal, H. Stambuk, J.C. Durack, C. T. Sofocleous, R.J.C. Meester, U. Wiesner, S. Patel, Clinically-translated silica nanoparticles as dual-modality cancer-targeted probes for image-guided surgery and interventions, Integr. Biol. 5 (2013) 74–86, https://doi.org/10.1039/c2ib20174g.
[170] E. Phillips, O. Penate-Medina, P.B. Zanzonico, R.D. Carvajal, P. Mohan, Y. Ye, J. Humm, M. Gonen, H. Kalaigian, H. Schoder, H.W. Strauss, S.M. Larson, U. Wiesner, M.S. Bradbury, Clinical translation of an ultrasmall inorganic optical-PET imaging nanoparticle probe, Sci. Transl. Med. 6 (2014), https://doi.org/10.1126/scitranslmed.3009524, 260ra149-260ra149.
[171] F. Farjadian, A. Roointan, S. Mohammadi-Samani, M. Hosseini, Mesoporous silica nanoparticles: synthesis, pharmaceutical applications, biodistribution, and biosafety assessment, Chem. Eng. J. 359 (2019) 684–705, https://doi.org/10.1016/j.cej.2018.11.156.
[172] R.K. Kankala, Y. Han, J. Na, C. Lee, Z. Sun, S. Wang, T. Kimura, Y.S. Ok, Y. Yamauchi, A. Chen, K.C.-W. Wu, Nanoarchitectured structure and surface biofunctionality of mesoporous silica nanoparticles, Adv. Mater. 32 (2020) 1907035, https://doi.org/10.1002/adma.201907035.
[173] M. Vallet-Regí, M. Colilla, I. Izquierdo-Barba, M. Manzano, Mesoporous silica nanoparticles for drug delivery: current insights, Molecules 23 (2017) 47, https://doi.org/10.3390/molecules23010047.
[174] J.-B. Coty, C. Vauthier, Characterization of nanomedicines: a reflection on a field under construction needed for clinical translation success, J. Contr. Release 275 (2018) 254–268, https://doi.org/10.1016/j.jconrel.2018.02.013.
[175] A.C. Anselmo, S. Mitragotri, A Review of clinical translation of inorganic nanoparticles, AAPS J. 17 (2015) 1041–1054, https://doi.org/10.1208/s12248-015-9780-2.
[176] Q. Lei, J. Guo, A. Noureddine, A. Wang, S. Wuttke, C.J. Brinker, W. Zhu, Sol-gel-based advanced porous silica materials for biomedical applications, Adv. Funct. Mater. (2020) 1909539, https://doi.org/10.1002/adfm.201909539.
[177] J. Shi, P.W. Kantoff, R. Wooster, O.C. Farokhzad, Cancer nanomedicine: progress, challenges and opportunities, Nat. Rev. Canc. 17 (2017) 20–37, https://doi.org/10.1038/nrc.2016.108.